Response to reviewer comments

Revisiting the global budget of atmospheric glyoxal: updates on terrestrial and marine precursor emissions, chemistry, and impacts on atmospheric oxidation capacity

Manuscript ID: egusphere-2025-5083

We thank the reviewers for their very helpful comments. In response, we have made the following major changes: (1) we re-ran all global GEOS-Chem simulations at 2.5° longitude × 2° latitude and all analyses to better represent the spatial distribution of atmospheric glyoxal; (2) extensively revised the discussion associated with the hypothetical secondary glyoxal source over the global oceans to clarify our intentions and to demonstrate the substantial uncertainties regarding that hypothetical source; and (3) added several diagnostics to the evaluate the impacts of the revised representation of precursor and glyoxal emissions and chemistry on atmospheric CO, ozone, SOA, and HO_2. We also revised the main text to improve clarity throughout. We responded to each specific comment in detail below. The reviewer comments are shown in blue. Our replies are shown in regular black text, and the modified text is shown in *italic black text*.

Response to Anonymous Referee #1:

R1.1 The present study reports on improved glyoxal simulations by updated secondary production pathways and by the introduction of an artificial marine glyoxal source. It is well written and easy to follow and the figures are well-chosen. I have to apologize that I am not a chemist, such that many of my questions might be fully attributed to missing knowledge from my side. My major concern relates to the proposed artificial marine glyoxal source. While other model updates to the glyoxal production chain are explained, quantified and discussed in great detail, the suggested artificial marine glyoxal source remains poorly justified in terms of realistic chemical candidates and potential real-world equivalents.

Thank you for your detailed review and valuable comments. Here, our goal is to estimate how large that hypothetical glyoxal source might be given satellite constraints, and whether that estimated source is consistent with independent measurements. The marine glyoxal source introduced in our study is hypothetical but is tentatively supported by *in situ* and ground-based remote sensing measurements. We revised the main text to make the hypothetical nature more evident to readers. We also added discussion to elucidate the observational support for this hypothesis and explore its uncertainties.

[Main text, Section 4.3]:

TROPOMI and other in situ and remote sensing measurements tentatively implied a secondary source of glyoxal over the tropical MBL associated with unknown, potentially biogenic, marine precursors. In this work, we used TROPOMI observations to estimate how large that hypothetical secondary glyoxal source might be, and we evaluated whether the inclusion of that hypothetical glyoxal source is consistent with independent in situ and remote sensing measurements in the global MBL. Previous studies have tentatively linked the glyoxal in the MBL to biologically active waters or to photochemical production from the dissolved organic matter (DOM) content in sea water. However, currently reported concentrations or fluxes of precursors (e.g., isoprene, ethylene, and propene) appear insufficient to explain the magnitude of glyoxal inferred from satellite observations (Broadgate et al., 2004; Zhang et al., 2025; Pound, 2021). In addition, measurements of NMVOCs in the MBL remain too sparse to provide a quantitative global constraint. We therefore interpret the inferred marine glyoxal source as a diagnostic term representing the glyoxal production from potentially missing marine NMVOCs.

[Main text, Conclusion]:

Our study highlights the need for improved measurement of VOCs in the MBL and for a deeper exploration of their photochemical transformations. Our exploratory addition

of a hypothetical secondary glyoxal source (66 Tg yr^{-1}) raised the global atmospheric glyoxal source to 106 Tg yr^{-1} and its burden to 39 Gg. While this addition shows tentative consistency with in situ MBL observations, this hypothetical glyoxal source cannot be explained by known marine precursor emissions. Recent work suggests marine biogenic emissions of precursors, such as isoprene, may be larger than previous estimates (Zhang et al., 2022). However, our evaluation of model results against limited aircraft measurements points to the possible influence of a more long-live precursor, the nature and impacts of which remain highly uncertain. Resolving this gap in marine photochemistry is essential for quantifying the roles of glyoxal and its precursors in marine and global atmospheric chemistry.

R1.2 At the same time, it has significant impact and causes an increase in the global glyoxal burden of over 100%. Do the authors assume this proposed marine glyoxal precursor to be uniformly distributed in the global marine surface?

Thank you for pointing out the lack of clarity regarding the spatial distribution of the hypothetical marine glyoxal source. In this study, we used the TROPOMI glyoxal observations to estimate a hypothetical secondary glyoxal source in the MBL. As such, that source is spatially distributed according to TROPOMI observations and the lifetime of glyoxal. We revised the main text to clarify this point. We also added Figure S1 to illustrate the spatial distribution of that hypothetical marine glyoxal source:

[Main text, Section 4.3]:

We estimated the potential secondary glyoxal source by hypothesizing a short-lived marine precursor, which was emitted at the sea surface, instantaneously mixed throughout the MBL, and oxidized by OH to produce glyoxal at 100% yield. We started by assuming an a priori daytime emission for this hypothetical precursor, scaled to

match the TROPOMI-observed glyoxal VCDs over the global ocean at 2.5° × 2° resolution:

...

This optimization was iterated twice until the simulated marine glyoxal VCDs agreed with satellite observations within 20%, yielding an estimated daytime secondary glyoxal source of 66 Tg yr^{-1} over the global oceans that spatially correlated with TROPOMI observations (Figures 7 and S3).

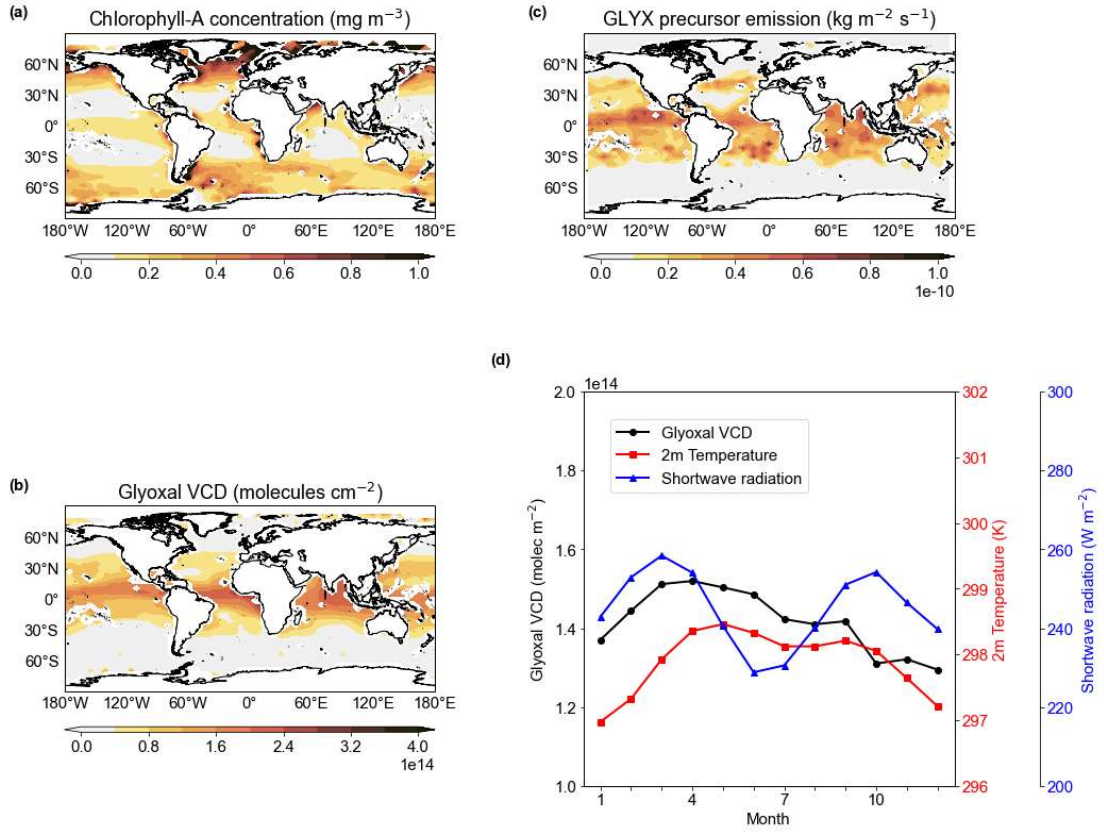

Figure S3. *(a) Annual mean chlorophyll-A concentrations in surface sea water retrieved by the MODIS instrument; (b) annual mean TROPOMI-observed glyoxal VCD over the ocean; (c) annual mean emissions of the hypothetical marine precursor of glyoxal as estimated in this study; (d) seasonal variation of TROPOMI-observed glyoxal VCD, 2-m air temperature, and surface downward shortwave radiation flux over the tropical ocean (30° S-30° N).*

R1.3 Where could it originate from and how realistic is it? The authors mention that previous literature suggested e.g. DOM as potential marine glyoxal source, but the study does not debate how their proposed artificial source relates to these findings.

Thank you for your comment. The origin of the hypothetical marine glyoxal source is yet unclear. Previous measurements showed that marine emissions of NMVOCs were mostly isoprene, ethylene, and propene. However, the reported concentrations or fluxes are insufficient to explain the magnitude of glyoxal inferred from satellite observations.

Reference	Measured marine NMVOC	Estimated flux or concentration in the MBL	Potential contribution to marine glyoxal
Zhang et al., 2025	Isoprene	1.2 Tg/yr	0.04Tg/yr
Ferracci et al. (2024)	Isoprene	0-500 ppt	< 20 ppt
Plass-Dulmer et al., (1995)	Ethylene	1 Tg/yr	0.2Tg/yr
Pound (2021)	Ethylene	25 ppt	< 5 ppt

We added discussions in the main text to show that (1) satellite-observed glyoxal abundance could not be explained by currently known precursors and their emissions, and (2) the lifetime of the unknown precursor maybe longer than previously thought. We also added a paragraph in the Conclusion section to highlight the unknown nature of that source and the need for further investigation.

[Main text, Section 4.3]: *TROPOMI and other in situ and remote sensing*

measurements tentatively implied a secondary source of glyoxal over the tropical MBL associated with unknown, potentially biogenic, marine precursors. In this work, we used TROPOMI observations to estimate how large that hypothetical secondary glyoxal source might be, and we evaluated whether the inclusion of that hypothetical glyoxal source is consistent with independent in situ and remote sensing measurements in the global MBL. Previous studies have tentatively linked the glyoxal in the MBL to biologically active waters or to photochemical production from the dissolved organic matter (DOM) content in sea water. However, currently reported concentrations or fluxes of precursors (e.g., isoprene, ethylene, and propene) appear insufficient to explain the magnitude of glyoxal inferred from satellite observations (Broadgate et al., 2004; Zhang et al., 2025; Pound, 2021). In addition, measurements of NMVOCs in the MBL remain too sparse to provide a quantitative global constraint. We therefore interpret the inferred marine glyoxal source as a diagnostic term representing the glyoxal production from potentially missing marine NMVOCs.

[Main text, Section 6]: *Figure S4 further compares the simulated glyoxal over the remote ocean with the aircraft observations from Volkamer et al. (2015) and Kluge et al. (2023). With the added marine glyoxal source, GC-TM-EC -simulated glyoxal concentrations aligned better with the limited aircraft data. However, the model overestimated glyoxal in surface air over the Northeast Pacific but underestimated it over the Atlantic. Additionally, the aircraft profiles suggested a more gradual decline in glyoxal concentration with altitude than simulated, which may indicate a longer-lived marine-derived precursor. This inference is inconsistent with the current understanding that marine-emitted VOCs are predominantly short-lived alkenes (e.g., ethylene and propene) and isoprene (Broadgate et al., 2004; Zhang et al., 2025; Pound, 2021).*

[Main text, Conclusion]: *Our study highlights the need for improved measurement of*

VOCs in the MBL and for a deeper exploration of their photochemical transformations. Our exploratory addition of a hypothetical secondary glyoxal source (66 Tg yr^{-1}) raised the global atmospheric glyoxal source to 106 Tg yr^{-1} and its burden to 39 Gg. While this addition shows tentative consistency with in situ MBL observations, this hypothetical glyoxal source cannot be explained by known marine precursor emissions. Recent work suggests marine biogenic emissions of precursors, such as isoprene, may be larger than previous estimates (Zhang et al., 2022). However, our evaluation of model results against limited aircraft measurements points to the possible influence of a more long-live precursor, the nature and impacts of which remain highly uncertain. Resolving this gap in marine photochemistry is essential for quantifying the roles of glyoxal and its precursors in marine and global atmospheric chemistry.

R1.4 Further, the impact of the proposed marine glyoxal source on related tropospheric tracers could be evaluated better. It is not clear to me how this new glyoxal chemistry impacts e.g. tropospheric CO or SOA formation and whether its impact on surface ozone is an improvement or degradation with respect to observations.

Thanks for this important suggestion. We added figures and diagnostics to evaluate the broader impacts of the revised representations of glyoxal and its precursors on surface CO, ozone, and SOA (Figure S7-S9). However, most of these changes were driven by the changes in terrestrial precursor emissions, particularly biogenic isoprene and biomass burning NMVOC emissions. The marine glyoxal source also had an impact on HO_2 concentrations in the remote marine atmosphere, which we demonstrated in Figure S6.

[Main text, Section 8]:

We also evaluated the broader influence of the revised glyoxal and precursors representations on tropospheric chemistry (Figures S7, S8, S9). Relative to the GC-CTRL simulation, increased precursor emissions in the GC-TM-EC simulation

substantially raised the global mean surface CO concentrations from 99.1 ppb to 113.5 ppb, reducing the model bias against MOPITT observations from -25% to 13% (Figure S7), especially over Eastern United States, East and South Asia, and the tropical South America and Africa. Similarly, enhanced terrestrial precursor emissions moderately increased the simulated global mean surface ozone concentration over land from 22.8 ppb in GC-CTRL to 29.5 ppb in GC-TM-EC, closer to the 34.1 ppb reported in the data -assimilated product of Wang et al., (2025) (Figure S8). The increased precursor emissions and atmospheric glyoxal abundance in the GC-T-EC experiment also led to a stronger heterogeneous uptake of glyoxal by aqueous particles, thereby enhancing SOA formation (Table 2). Over China, for example, the GC-T-EC experiment simulated significantly higher SOA concentrations than the GC-CTRL experiment, especially at suburban and remote sites (Figure S9). These increases brought simulations closer to—though still substantially below—observed concentrations, indicating that SOA formation involves complex mechanisms beyond glyoxal chemistry (Miao et al., 2021). The apparent improvements in simulated CO, ozone, and SOA should therefore be interpreted as supporting the chemical plausibility of the revised glyoxal budget and underscoring glyoxal's role as a proxy for atmospheric NMVOC emissions.

[Main text, Section 8]:

Figure S6 compares our simulated HO_x vertical profile against the observations in the marine boundary layer (below 2,500 m) during the ATom-2 mission (Brune et al., 2020). The OH concentrations simulated in the GC-CTRL simulation agreed well with observations, and our improved glyoxal simulation did not significantly change the OH profile over the remote ocean. The HO_2 concentration simulated in GC-TM-EC slightly alleviated the underestimation in GC-TM-E *by 5% but still underestimated HO_2compared to the observations, indicating the potential lack or persistent underestimation of HO_2 sources (e.g., OVOCs) over the remote MBL.*

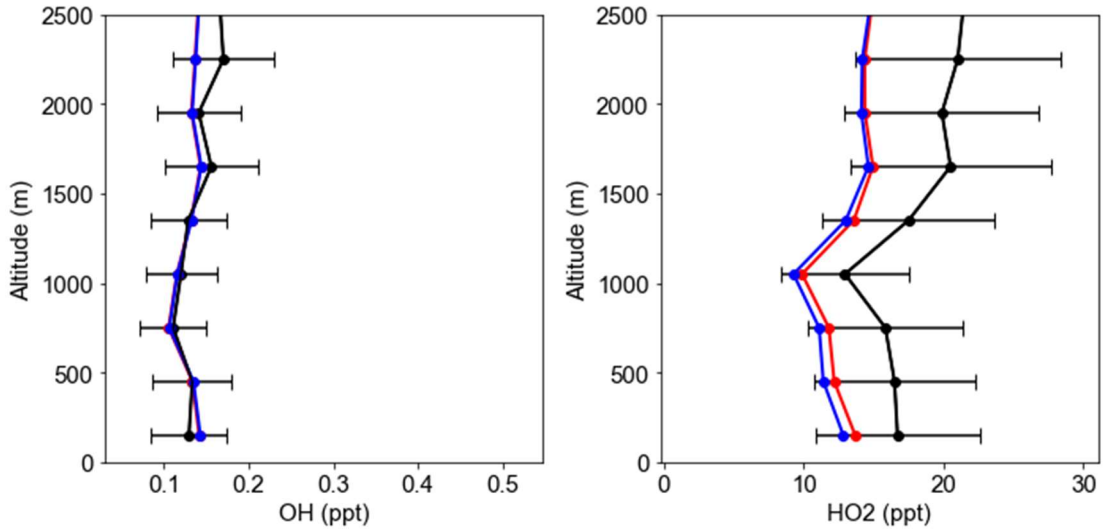

Figure S6. *The vertical profiles of ATom-2 aircraft measurements over the tropical ocean (20◦S-20◦N) and corresponding simulated OH and HO_2 concentration (GC-CTRL in blue; GC-TM-EC in red) within the MBL.*

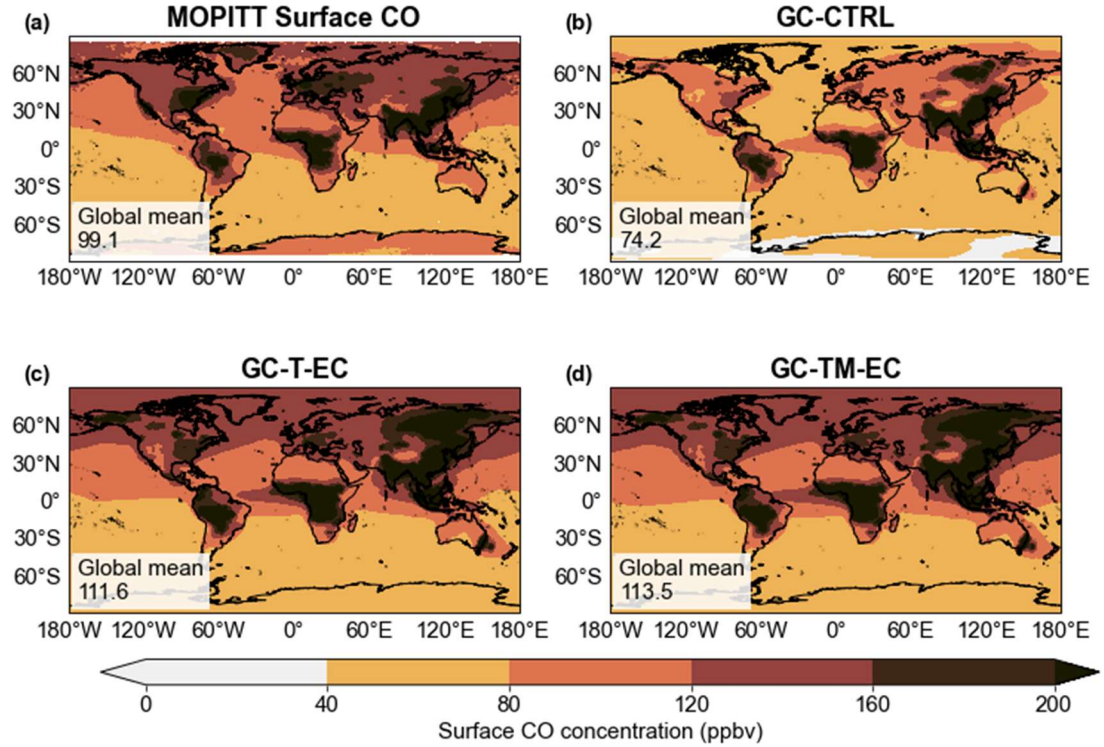

Figure S7. *The annual mean (a) MOPITT-retrieved surface CO concentrations and simulated surface CO concentration in the (b) GC-CTRL, (c) GC-T-EC and (d) GC-TM-EC experiments (unit: ppb) from July 2019 to June 2020. For MOPITT, the annual mean surface CO was derived from the average of the daytime and nighttime retrievals,*

corresponding to approximately 10:30 and 22:30 local time, respectively.

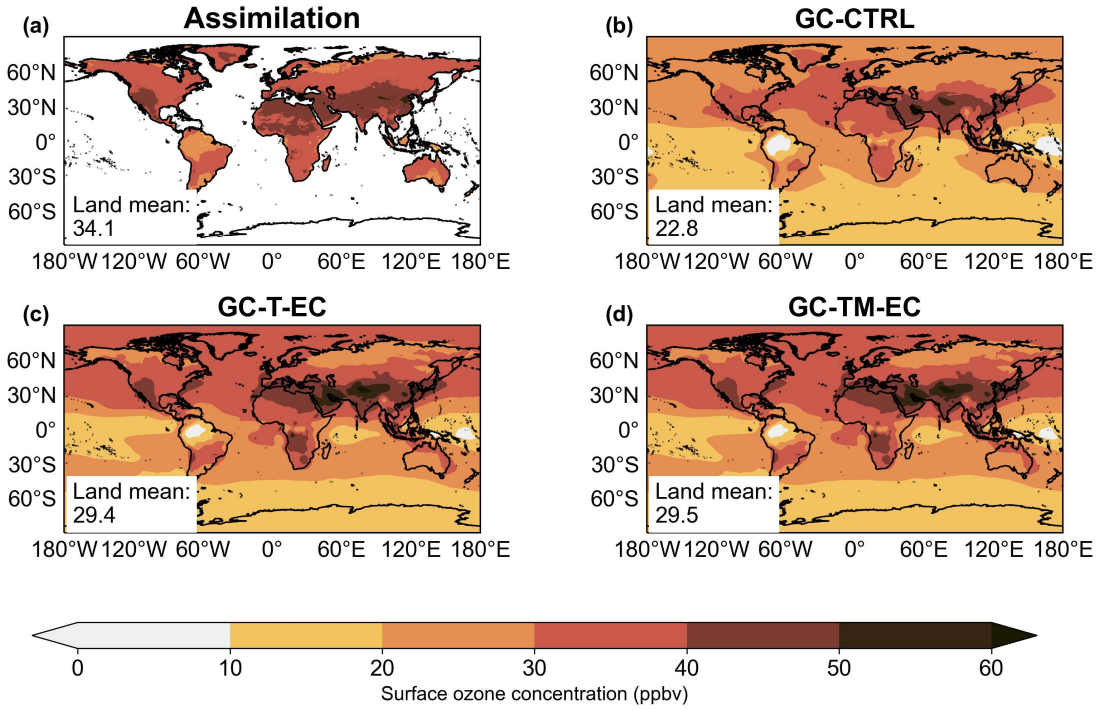

Figure S8. *The annual mean (a) assimilated global surface ozone concentrations over land (Wang et al., 2025) and simulated surface ozone concentrations in the (b) GC-CTRL, (c) GC-T-EC and (d) GC-TM-EC experiments (unit: ppb) from July 2019 to June 2020.*

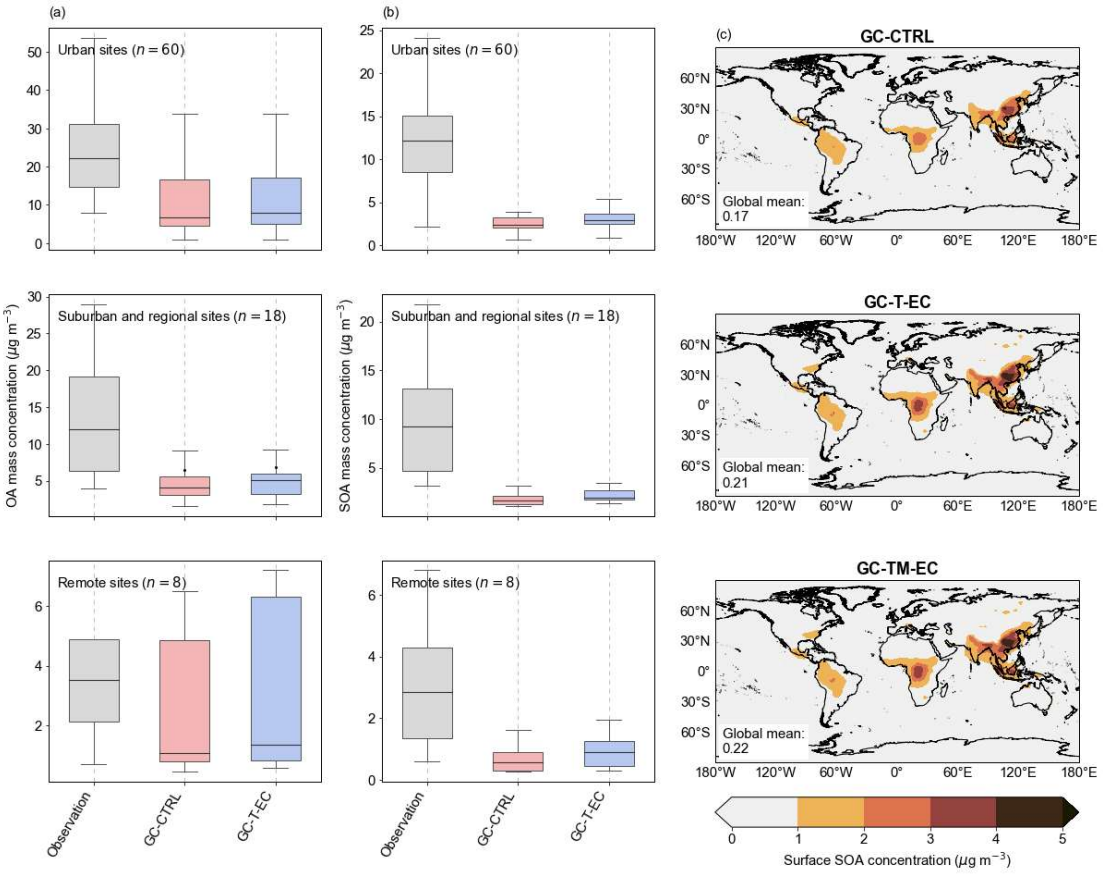

Figure S9 *Evaluations of GEOS-Chem simulated (a) OA and (b) SOA against the measurements summarized by Miao et al. (2021) in China. In each boxplot, the horizontal line marks the median, the box represents the interquartile range (25th to 75th percentiles). The whiskers indicate the spread of the corresponding observations and simulations. (c) The simulated annual mean surface SOA concentration in GC-CTRL, GC-T-EC and GC-TM-EC (unit: μg m^{-3}) from July 2019 to June 2020.*

Other comments:

R1.5 Section 3: The evaluation of the simulations with respect to surface and airborne observations remains a bit unclear. I suggest to name and discuss potential biases introduced by missing spatial and timely correlation between the observations and the simulations.

It is not clear from the text whether the comparison to ground- and airborne

observations considers any time correlation or, instead, is performed using the previously discussed yearly averaged simulations (which would introduce systematic biases that might cause part of the negative model bias).

Thank you for pointing out the lack of clarity. For all model-observation comparisons, we sampled the model results at the location of the observation and during the month of the observation. We added these protocols to the main text. We also acknowledge that some measurements may be influenced by local urban or biomass burning emissions, which may not be resolved in our simulations at 2.5° x 2° resolution.

[Main text, Section 2.4]: *We also compared simulated glyoxal concentrations against surface, ship-based, and aircraft measurements of glyoxal over land and ocean. Table S1 compiles the measurements reported in the literature. To compare model results against observations, the monthly mean simulated glyoxal concentrations were sampled at the coordinates of the measurement site and during the month of measurement.*

[Main text, Section 3]: *Figure 2 evaluated the simulated concentrations of glyoxal against individual ground-based and aircraft measurements over land (Table S1). Some measurements were made in urban areas or areas affected by local biomass burning (Table S1) and could not be reproduced by our simulations at coarse resolution. However, even with these outliers excluded, the model still showed substantial underestimations of glyoxal concentrations compared to measurements at the surface and in the boundary layer (NMB = -90%), suggesting systematic errors in precursor emissions and/or near-surface chemistry.*

R1.6 It is also unclear how the altitudinal resolution of the simulations impacts the comparison to airborne observations. I understand that the comparison only considers observations at the surface and within the PBL. However, the vertical bVOC profile has a very pronounced vertical gradient in particular in the

lowermost troposphere. Or is the model bias constant throughout the PBL and the same for ground and airborne observations? Since the study concludes on missing (marine) surface sources, I would expect the model bias to be somewhat altitude dependent. The analysis might benefit from 1. clearly discussing the underlying methodology and potential thereoff resulting systematic biases 2. differentiating ground and airborne observations to enable a discussion of the altitudinal dependence of the model bias. For the latter, I suggest to add a figure with a comparison of glyoxal vertical profiles.

Thank you for this important comment. To address this concern, we added Figure S4 and explicit discussions on the observed and simulated vertical profiles of glyoxal over the oceans. We showed that the addition of the hypothetical marine glyoxal source helped alleviated the bias against aircraft measured vertical profile. However, there were substantial regional differences in the model performance, and the aircraft measurements tentatively indicated that the precursor of glyoxa in the marine air may be more long-lived than previously thought.

[Main text, Section 6]: *Figure S4 further compares the simulated glyoxal over the remote ocean with the aircraft observations from Volkamer et al. (2015) and Kluge et al. (2023). With the added marine glyoxal source, GC-TM-EC -simulated glyoxal concentrations aligned better with the limited aircraft data. However, the model overestimated glyoxal in surface air over the Northeast Pacific but underestimated it over the Atlantic. Additionally, the aircraft profiles suggested a more gradual decline in glyoxal concentration with altitude than simulated, which may indicate a longer-lived marine-derived precursor. This inference is inconsistent with the current understanding that marine-emitted VOCs are predominantly short-lived alkenes (e.g., ethylene and propene) and isoprene (Broadgate et al., 2004; Zhang et al., 2025; Pound, 2021).*

[Main text, Conclusion]: *Our study highlights the need for improved measurement of*

VOCs in the MBL and for a deeper exploration of their photochemical transformations. Our exploratory addition of a hypothetical secondary glyoxal source (66 Tg yr^{-1}) raised the global atmospheric glyoxal source to 106 Tg yr^{-1} and its burden to 39 Gg. While this addition shows tentative consistency with in situ MBL observations, this hypothetical glyoxal source cannot be explained by known marine precursor emissions. Recent work suggests marine biogenic emissions of precursors, such as isoprene, may be larger than previous estimates (Zhang et al., 2022). However, our evaluation of model results against limited aircraft measurements points to the possible influence of a more long-live precursor, the nature and impacts of which remain highly uncertain. Resolving this gap in marine photochemistry is essential for quantifying the roles of glyoxal and its precursors in marine and global atmospheric chemistry.

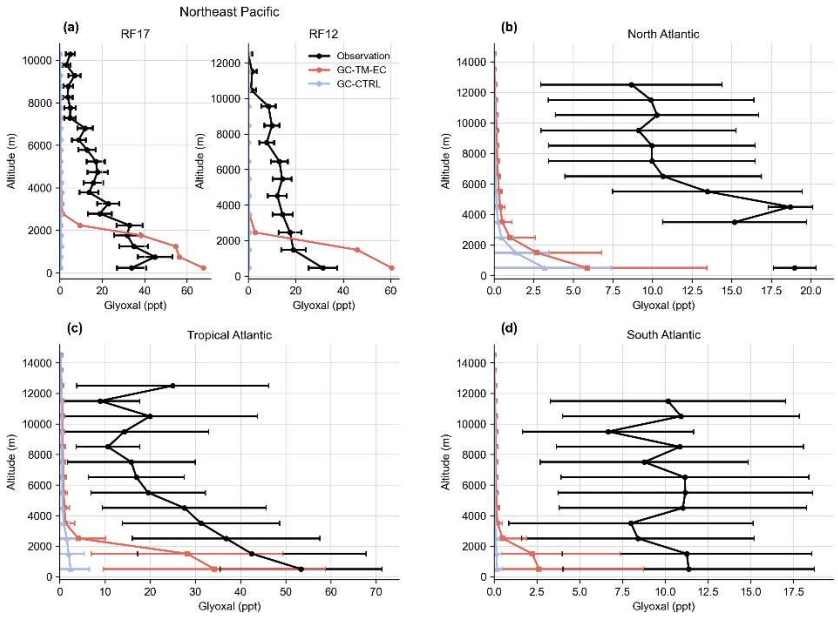

Figure S4. *Observed (black) and simulated vertical profiles of glyoxal (a) over the Northeast Pacific during two flights RF17 and RF12 as reported by Volkamer et al. (2015), and over (b) the North Atlantic, (c) the Tropical Atlantic, and (d) the South Atlantic during multiple flights as reported by Kluge et al. (2023). Simulated results from the GC-CTRL (blue) and GC-TM-EC (red) experiments were sampled at the coordinates of the measurements during the month of measurements. Whiskers indicate standard deviations within each vertical layer.*

R1.7 Section 8: This discussion might benefit from an evaluation with respect to

observations. Without, the results are a bit difficult to interpret. Is there any impact on tropospheric CO? Does the updated glyoxal burden only reflect on surface concentrations, or is there any impact in the free and upper troposphere? For all key tropospheric species, do the updated simulations improve or degrade the model bias with respect to observations? For example, what does the observed increase in surface ozone mean in terms of validation vs. observations? The resulting increase in SOA that the abstract reports on is not discussed. How does this relate to other studies and observations?

Thanks for this important suggestion. We added figures and diagnostics to evaluate the broader impacts of the revised representations of glyoxal and its precursors on surface CO, ozone, and SOA (Figures S7-S9). However, most of these changes were driven by the changes in terrestrial precursor emissions, particularly biogenic isoprene and biomass burning NMVOC emissions. We emphasized this point in the main text. The marine glyoxal source also had an impact on HO_2 concentrations in the remote marine atmosphere, which we also demonstrated in Figure S6.

[Main text, Section 8]:

We also evaluated the broader influence of the revised glyoxal and precursors representations on tropospheric chemistry (Figures S7, S8, S9). Relative to the GC-CTRL simulation, increased precursor emissions in the GC-TM-EC simulation substantially raised the global mean surface CO concentrations from 99.1 ppb to 113.5 ppb, reducing the model bias against MOPITT observations from -25% to 13% (Figure S7), especially over Eastern United States, East and South Asia, and the tropical South America and Africa. Similarly, enhanced terrestrial precursor emissions moderately increased the simulated global mean surface ozone concentration over land from 22.8 ppb in GC-CTRL to 29.5 ppb in GC-TM-EC, closer to the 34.1 ppb reported in the data-assimilated product of Wang et al., (2025) (Figure S8). The increased precursor

emissions and atmospheric glyoxal abundance in the GC-T-EC experiment also led to a stronger heterogeneous uptake of glyoxal by aqueous particles, thereby enhancing SOA formation (Table 2). Over China, for example, the GC-T-EC experiment simulated significantly higher SOA concentrations than the GC-CTRL experiment, especially at suburban and remote sites (Figure S9). These increases brought simulations closer to—though still substantially below—observed concentrations, indicating that SOA formation involves complex mechanisms beyond glyoxal chemistry (Miao et al., 2021). The apparent improvements in simulated CO, ozone, and SOA should therefore be interpreted as supporting the chemical plausibility of the revised glyoxal budget and underscoring glyoxal's role as a proxy for atmospheric NMVOC emissions.

[Main text, Section 8]:

Figure S6 compares our simulated HO_x vertical profile against the observations in the marine boundary layer (below 2,500 m) during the ATom-2 mission (Brune et al., 2020). The OH concentrations simulated in the GC-CTRL simulation agreed well with observations, and our improved glyoxal simulation did not significantly change the OH profile over the remote ocean. The HO_2 concentration simulated in GC-TM-EC slightly alleviated the underestimation in GC-TM-E *by 5% but still underestimated HO_2compared to the observations, indicating the potential lack or persistent underestimation of HO_2 sources (e.g., OVOCs) over the remote MBL.*

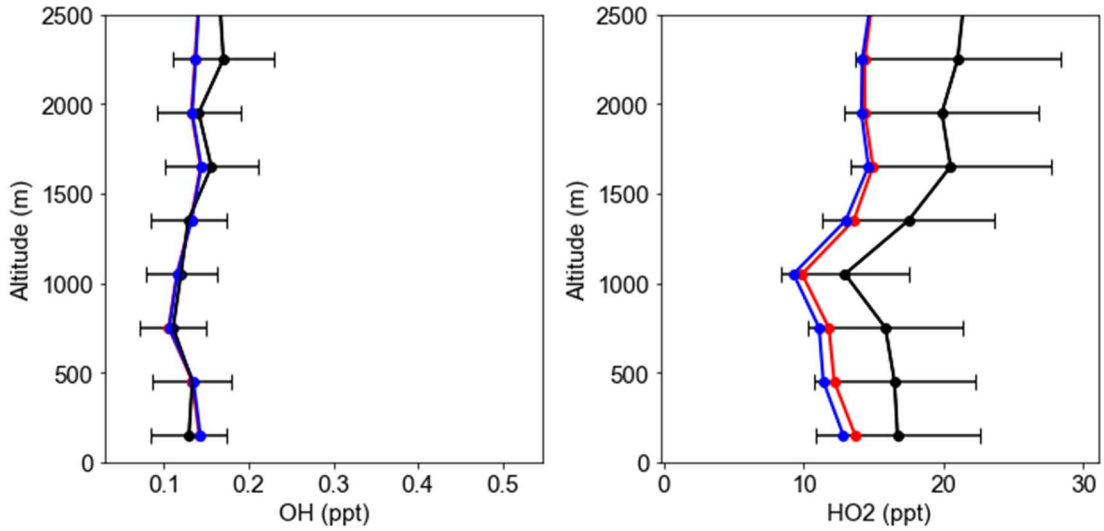

Figure S6. *The vertical profiles of ATom-2 aircraft measurements over the tropical ocean (20◦S-20◦N) and corresponding simulated OH and HO_2 concentration (GC-CTRL in blue; GC-TM-EC in red) within the MBL.*

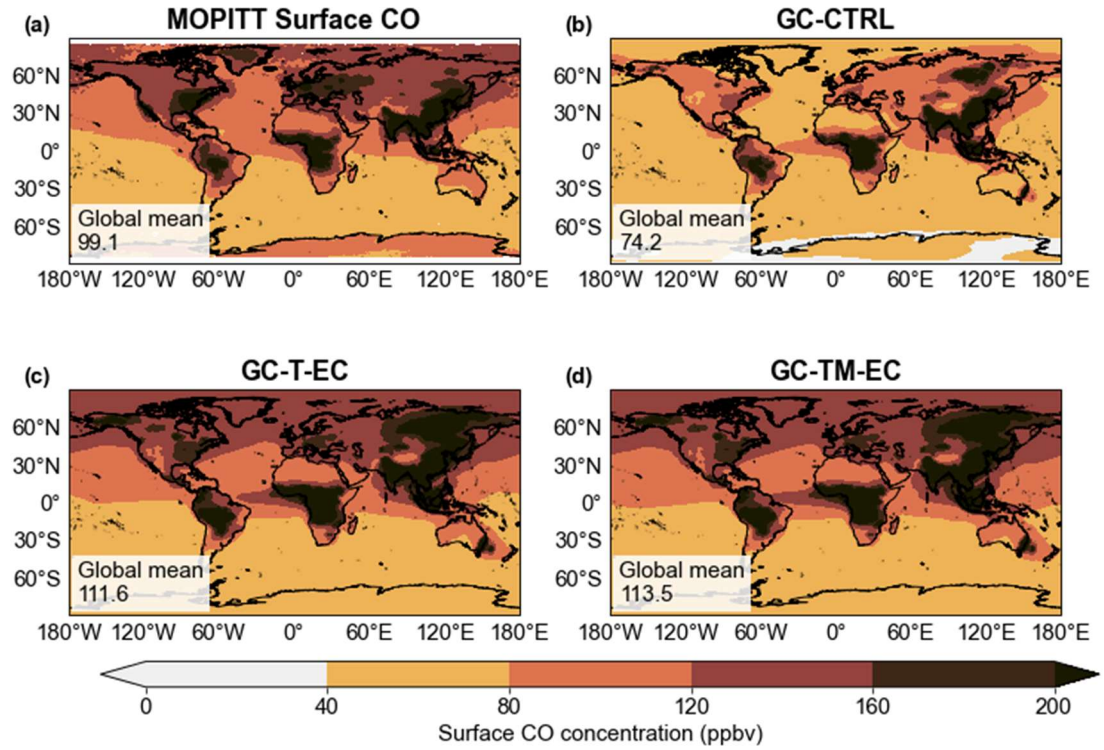

Figure S7 *The annual mean (a) MOPITT-retrieved surface CO concentrations and simulated surface CO concentration in the (b) GC-CTRL, (c) GC-T-EC and (d) GC-TM-EC experiments (unit: ppb) from July 2019 to June 2020. For MOPITT, the annual mean surface CO was derived from the average of the daytime and nighttime retrievals,*

corresponding to approximately 10:30 and 22:30 local time, respectively.

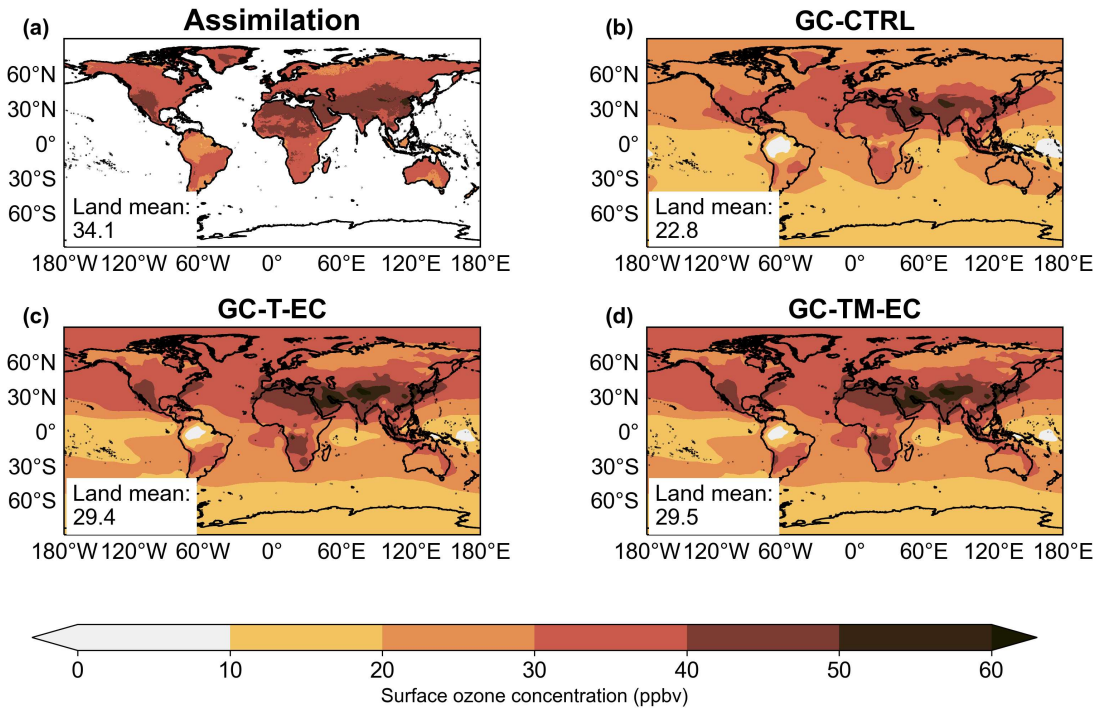

Figure S8. *The annual mean (a) assimilated global surface ozone concentrations over land (Wang et al., 2025) and simulated surface ozone concentrations in the (b) GC-CTRL, (c) GC-T-EC and (d) GC-TM-EC experiments (unit: ppb) from July 2019 to June 2020.*

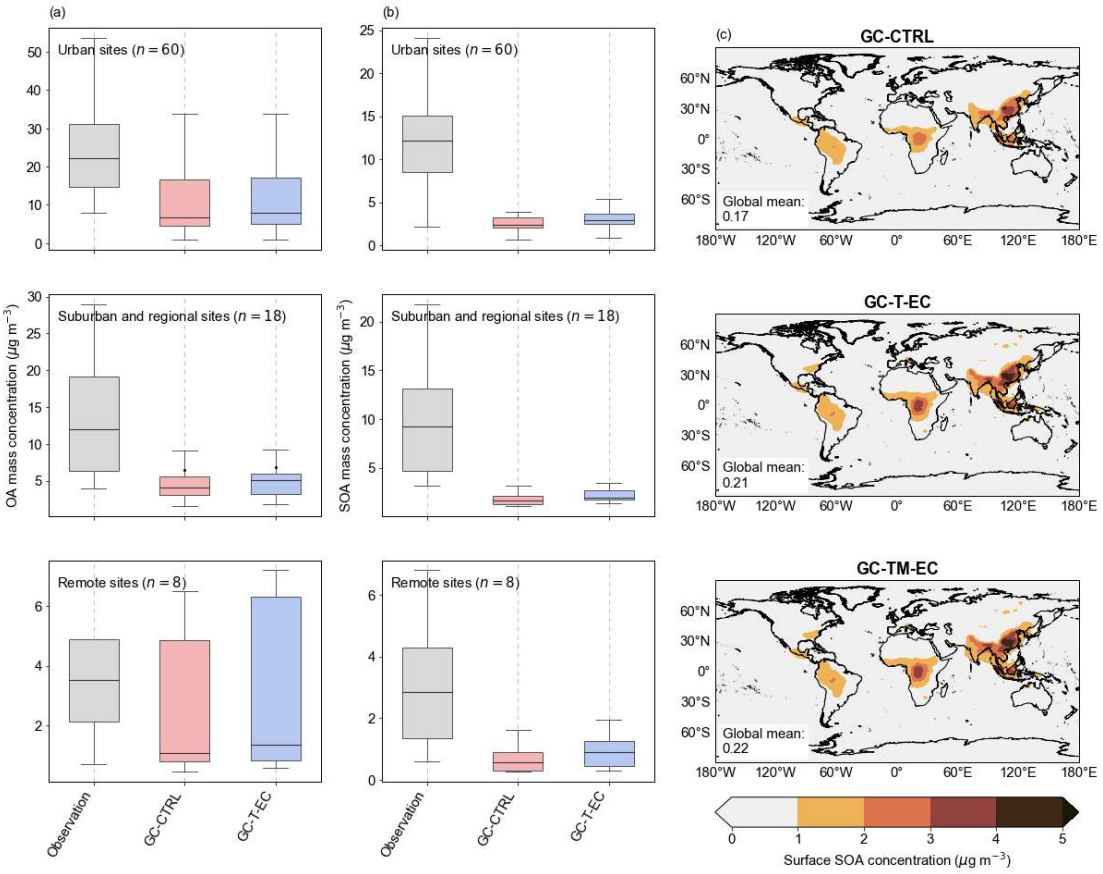

Figure S9. *Evaluations of GEOS-Chem simulated (a) OA and (b) SOA against the measurements summarized by Miao et al. (2021) in China. In each boxplot, the horizontal line marks the median, the box represents the interquartile range (25th to 75th percentiles). The whiskers indicate the spread of the corresponding observations and simulations. (c) The simulated annual mean surface SOA concentration in GC-CTRL, GC-T-EC and GC-TM-EC (unit: μg m^{-3}) from July 2019 to June 2020.*

Minor comments:

R1.8 Lines 9-10: I imagine the increase in ozone and SOA must be significantly larger than the global mean over some regions. How does this compare to observations?

Thank you for this important comment. We added figures and diagnostics to evaluate

the broader impacts of the revised representations of glyoxal and its precursors on surface CO, ozone, and SOA (Figures S7-S9) and the spatial distribution of those impacts. Most of these changes were driven by the changes in terrestrial precursor emissions, particularly biogenic isoprene and biomass burning NMVOC emissions. We emphasized this point in the main text.

[Main text, Section 8]:

We also evaluated the broader influence of the revised glyoxal and precursors representations on tropospheric chemistry (Figures S7, S8, S9). Relative to the GC-CTRL simulation, increased precursor emissions in the GC-TM-EC simulation substantially raised the global mean surface CO concentrations from 99.1 ppb to 113.5 ppb, reducing the model bias against MOPITT observations from -25% to 13% (Figure S7), especially over Eastern United States, East and South Asia, and the tropical South America and Africa. Similarly, enhanced terrestrial precursor emissions moderately increased the simulated global mean surface ozone concentration over land from 22.8 ppb in GC-CTRL to 29.5 ppb in GC-TM-EC, closer to the 34.1 ppb reported in the data-assimilated product of Wang et al., (2025) (Figure S8). The increased precursor emissions and atmospheric glyoxal abundance in the GC-T-EC experiment also led to a stronger heterogeneous uptake of glyoxal by aqueous particles, thereby enhancing SOA formation (Table 2). Over China, for example, the GC-T-EC experiment simulated significantly higher SOA concentrations than the GC-CTRL experiment, especially at suburban and remote sites (Figure S9). These increases brought simulations closer to—though still substantially below—observed concentrations, indicating that SOA formation involves complex mechanisms beyond glyoxal chemistry (Miao et al., 2021). The apparent improvements in simulated CO, ozone, and SOA should therefore be interpreted as supporting the chemical plausibility of the revised glyoxal budget and underscoring glyoxal's role as a proxy for atmospheric NMVOC emissions.

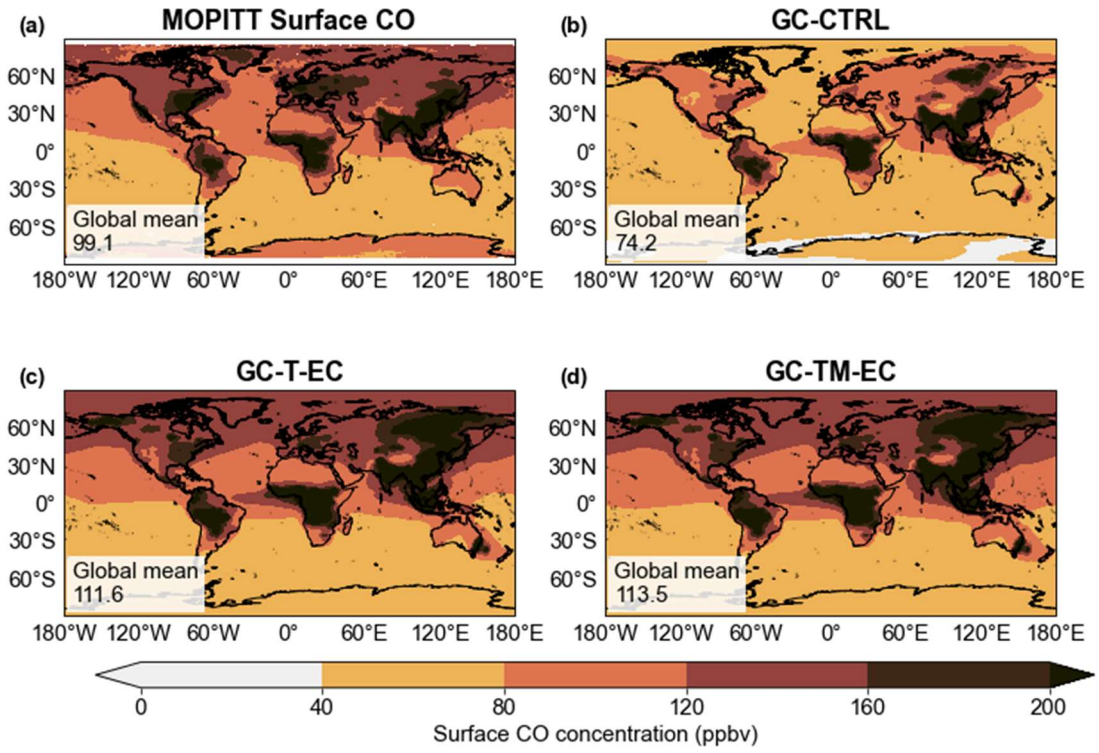

Figure S7. *The annual mean (a) MOPITT-retrieved surface CO concentrations and simulated surface CO concentration in the (b) GC-CTRL, (c) GC-T-EC and (d) GC-TM-EC experiments (unit: ppb) from July 2019 to June 2020. For MOPITT, the annual mean surface CO was derived from the average of the daytime and nighttime retrievals, corresponding to approximately 10:30 and 22:30 local time, respectively.*

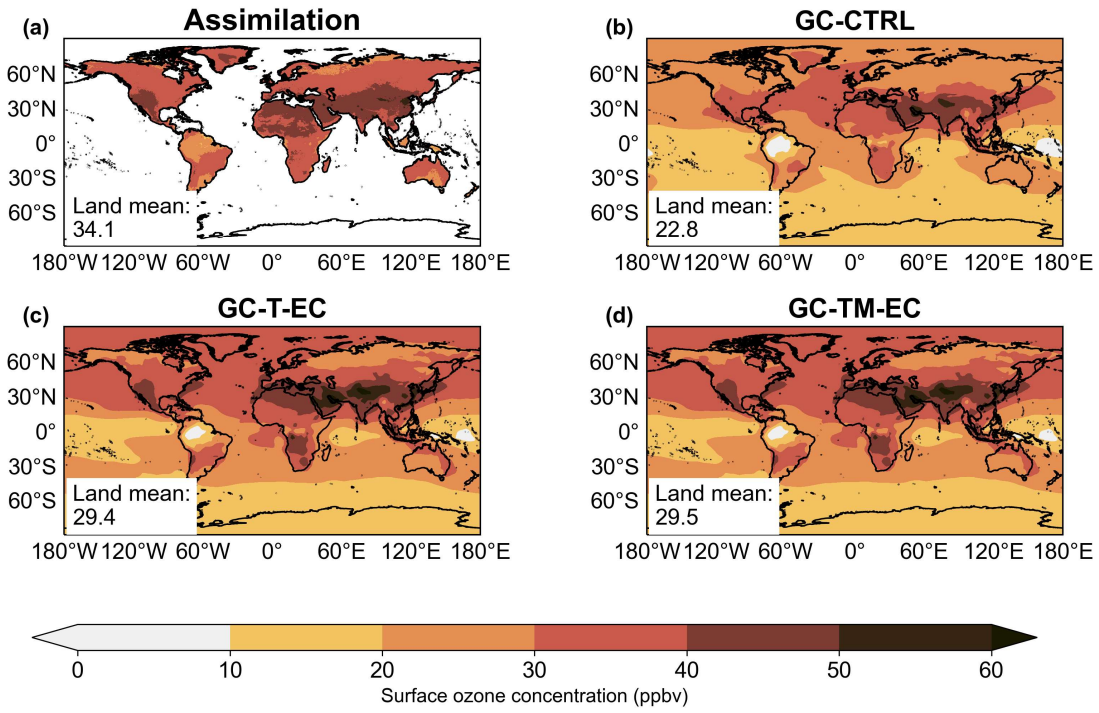

Figure S8. *The annual mean (a) assimilated global surface ozone concentrations over land (Wang et al., 2025) and simulated surface ozone concentrations in the (b) GC-CTRL, (c) GC-T-EC and (d) GC-TM-EC experiments (unit: ppb) from July 2019 to June 2020.*

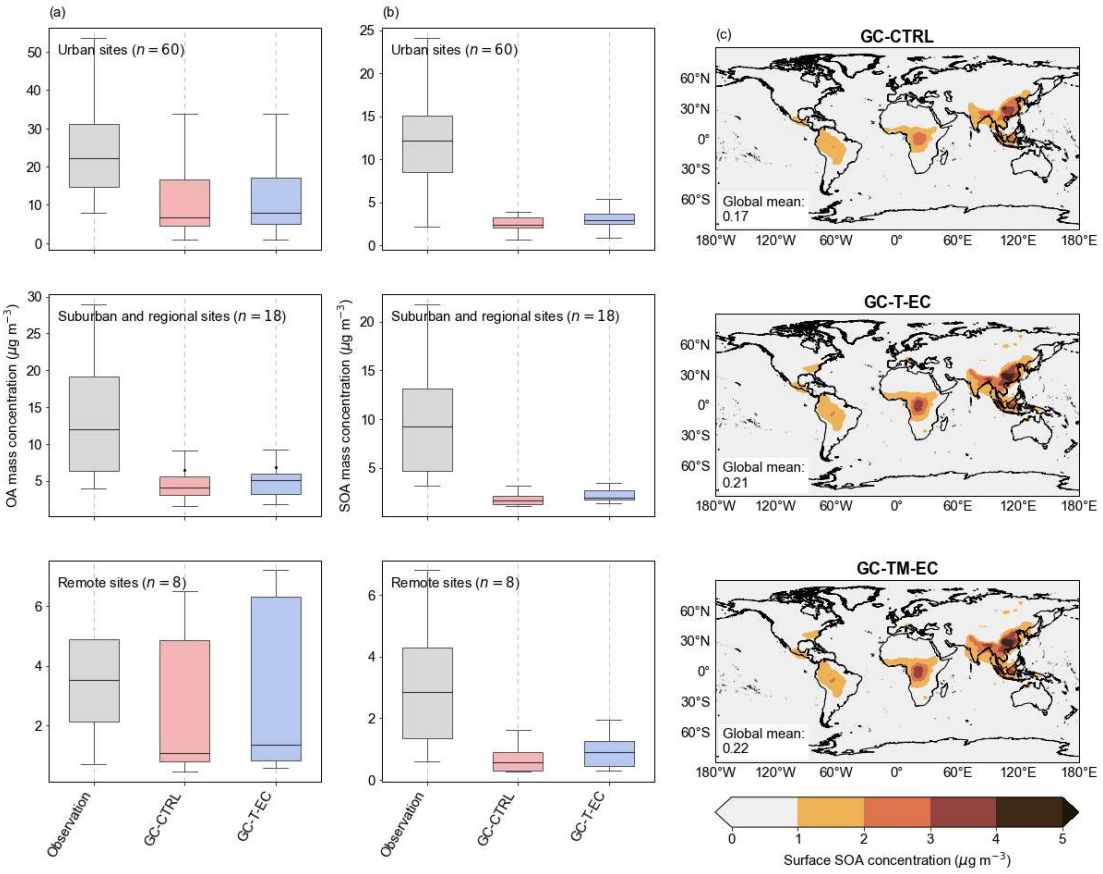

Figure S9. *Evaluations of GEOS-Chem simulated (a) OA and (b) SOA against the measurements summarized by Miao et al. (2021) in China. In each boxplot, the horizontal line marks the median, the box represents the interquartile range (25th to 75th percentiles). The whiskers indicate the spread of the corresponding observations and simulations. (c) The simulated annual mean surface SOA concentration in GC-CTRL, GC-T-EC and GC-TM-EC (unit: μg m^{-3}) from July 2019 to June 2020.*

R1.9 Line 24: column concentrations -> is this supposed to be slant column density or vertical column density? I suggest to use the common scientific term throughout the manuscript

Thank you for pointing out this error. We now consistently refer to the glyoxal vertical column density (VCD) throughout the text. For example:

[Main text, Section 2.4]: *We used the tropospheric glyoxal vertical column densities*

(VCDs) observed by the TROPOspheric Monitoring Instrument (TROPOMI) during July 2019 to June 2020 to evaluate our global atmospheric glyoxal simulations and to infer the magnitude of a hypothetical secondary glyoxal source in the MBL (Section 4.3).

...

The glyoxal SCDs were then converted to tropospheric VCDs using air mass factors (AMFs), accounting for the radiative transfer through the atmosphere (Palmer et al., 2001).

R1.10 Line 25: missing space

We revised this sentence. Thank you.

[Main text, Introduction]: *In addition, satellite observations of tropospheric glyoxal column concentrations serve as a proxy for NMVOC emissions, offering precursor-differentiating information when analyzed in combination with formaldehyde, another widely used proxy.*

R1.11 Line 35: I suggest to include more recent studies, e.g. using TROPOMI observations

Thank you for the suggestions. We added a most recent study (Sfendla et al., 2026) that inversely estimated global glyoxal budget based on TROPOMI data:

[Main text, Introduction]: *More recently, Sfendla et al. (2026) used TROPOMI satellite observations to inversely derive an 110 Tg yr^{-1} global terrestrial source for atmospheric glyoxal. However, over 40% of this inferred terrestrial source could not be accounted for by known precursors and chemical mechanisms, highlighting the persistent gap of in our understanding of atmospheric glyoxal sources.*

R1.12 Line 151: This is probably explained in detail in the respective references, but since the present study explicitly explores the impact of updated glyoxal production on e.g. surface ozone, I wonder about the assumptions made regarding the a priori glyoxal profiles in the satellite retrievals. This is even more crucial with respect to the discussed marine surface glyoxal production and resulting concentrations, since in particular the marine glyoxal profiles are quite uncertain over many regions.

Thank you for pointing out this omission. We added explicit statements regarding the *a priori* vertical profiles used in the TROPOMI glyoxal retrievals. We also added Figure S4 to diagnose the simulated glyoxal profile in our updated glyoxal model including the hypothetical marine glyoxal source, with discussions on the implications of the model-observation comparison

[Main text, Section 2.4]: *Over land, the TROPOMI retrievals used the a priori glyoxal profiles simulated by the Model of Atmospheric composition at Global and Regional scales using Inversion Techniques for Trace gas Emissions (MAGRITTE v1.1, Müller et al., (2019)). Over oceans, a fixed parameterized glyoxal profile based on aircraft observations over the tropical Pacific from Volkamer et al., (2015) was used in the retrieval (Lerot et al., 2021a).*

[Main text, Section 6]: *Figure S4 further compares the simulated glyoxal over the remote ocean with the aircraft observations from Volkamer et al. (2015) and Kluge et al. (2023). With the added marine glyoxal source, GC-TM-EC-simulated glyoxal concentrations aligned better with the limited aircraft data. However, the model overestimated glyoxal in surface air over the Northeast Pacific but underestimated it over the Atlantic. Additionally, the aircraft profiles suggested a more gradual decline in glyoxal concentration with altitude than simulated, which may indicate a longer-lived marine-derived precursor. This inference is inconsistent with the current understanding that marine-emitted VOCs are predominantly short-lived alkenes (e.g., ethylene and propene) and isoprene (Broadgate et al., 2004; Zhang et al., 2025; Pound, 2021).*

[Main text, Conclusion]: *Our study highlights the need for improved measurement of VOCs in the MBL and for a deeper exploration of their photochemical transformations. Our exploratory addition of a hypothetical secondary glyoxal source (66 Tg yr^{-1}) raised the global atmospheric glyoxal source to 106 Tg yr^{-1} and its burden to 39 Gg. While this addition shows tentative consistency with in situ MBL observations, this hypothetical glyoxal source cannot be explained by known marine precursor emissions. Recent work suggests marine biogenic emissions of precursors, such as isoprene, may be larger than previous estimates (Zhang et al., 2022). However, our evaluation of model results against limited aircraft measurements points to the possible influence of a more long-live precursor, the nature and impacts of which remain highly uncertain. Resolving this gap in marine photochemistry is essential for quantifying the roles of glyoxal and its precursors in marine and global atmospheric chemistry.*

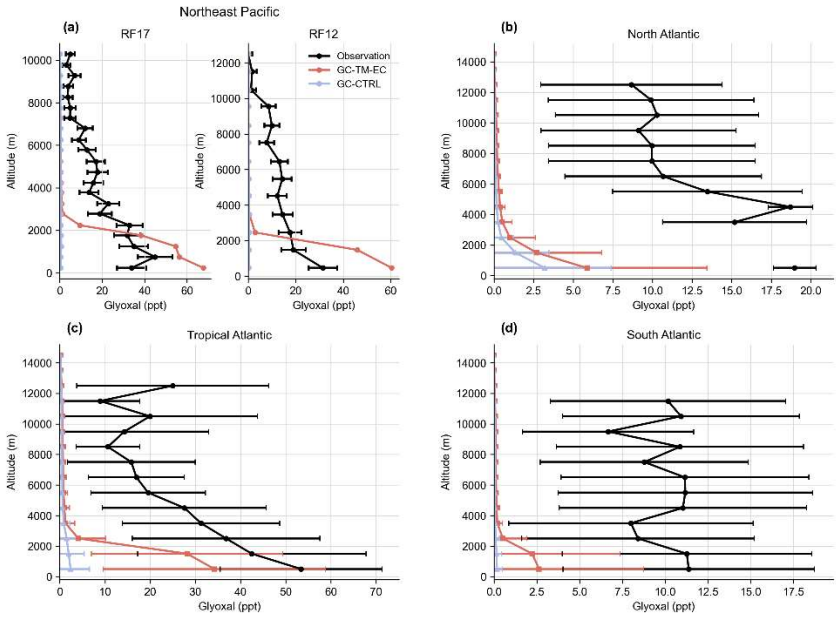

Figure S4. *Observed (black) and simulated vertical profiles of glyoxal (a) over the Northeast Pacific during two flights RF17 and RF12 as reported by Volkamer et al. (2015), and over (b) the North Atlantic, (c) the Tropical Atlantic, and (d) the South Atlantic during multiple flights as reported by Kluge et al. (2023). Simulated results*

from the GC-CTRL (blue) and GC-TM-EC (red) experiments were sampled at the coordinates of the measurements during the month of measurements. Whiskers indicate standard deviations within each vertical layer.

R1.13 Line 176: It is not clear how the yearly average is computed. I assume only simulations from the local satellite overpass time are used? This could be mentioned in the text, since otherwise the pronounced diurnal cycle of glyoxal might introduce systematic biases in the comparison. Also, for a species of such low optical density, the satellite must observe a significant fraction of negative retrievals. How are these taken into account in the comparison to a deterministic model?

Thank you for pointing out these critical omissions. We added details of the TROPOMI data averaging and the model sampling protocol for comparison to observations. We also specified that the model-observation comparison in Figure 1 was sampled at satellite overpass time (13:30 local time):

[Main text, Section 2.4]: *The TROPOMI Level 3 monthly mean glyoxal product averaged the native pixels to 0.05 º resolution after excluding pixels with quality assurance values less than 0.5 (Lerot et al., 2021b). This Level 3 product has shown better consistency with ground-based measurements and more reliable seasonal variation and local enhancements over regions of strong biogenic, anthropogenic, and biomass burning emissions, compared to earlier satellite retrievals vals (Lerot et al., 2021a). We regridded the Level 3 product to 2.5º longitude × 2º latitude for comparison with GEOS-Chem results and for inferring the hypothetical marine source of glyoxal (Section 4.3). Model results were sampled at the satellite overpass time. Even after the quality assurance filter, the Level 3 product showed small negative values over remote oceans and deserts where simulated glyoxal VCDs were also very small; these values were retained in the regridding.*

[Main text, Section 3]: *Figure 1 compares the annual mean tropospheric glyoxal VCDs at satellite overpass time (13:30 local time) from sensitivity experiments with TROPOMI observations and the standard GEOS-Chem simulation (GC-CTRL).*

[Figure 1 caption]: ***Figure 1.*** *Annual mean (July 2019–June 2020) atmospheric glyoxal column concentrations as (a) observed by TROPOMI, and as simulated in the (b) GC-CTRL, (c) GC-TM-E, (d) GC-T-EC, and (e) GC-TM-EC experiments. Model statistics against the TROPOMI observations over land, ocean, and globally are shown on the side of panels (b) to (e). The simulated VCDs were sampled at the daily satellite overpass time (13:30 local time) and then averaged to annual means.*

R1.14 Table S1. Without clarification of the measurements altitudes, the given glyoxal concentrations are difficult to interpret. The first column sometimes mentions a geographic region and sometimes what appears to be measurement campaign acronyms. It might help the reader to be concise. Also, please carefully check the literature references. Wendisch et al., (2016) does not at all report on glyoxal.

Thank you for the suggestion. We have clarified in the revised Table S1 that the reported values represent surface glyoxal concentrations unless otherwise noted. For comparisons with aircraft measurements, the corresponding note included "0–2 km mean" referring to a typical daytime PBL height. We also revised the first column of Table S1 to explicitly state the location of the reported measurement.

In addition, we thank the reviewer for pointing out the issue with the Wendisch et al. (2016) reference. While Wendisch et al. (2016) summarized the ACRIDICON-CHUVA campaign, the glyoxal retrieval based on that campaign were directly reported by Kluge et al. (2020). We have therefore replaced the reference accordingly. We checked all references listed in Table S1 to ensure that they directly reported the glyoxal observations used in this work. We also

corrected a misplaced parenthesis in reference 45 (Huang et al., 2023). The revised Table S1 and its notes are shown below.

Table S1. Observed surface or boundary layer mean glyoxal concentration over land and ocean. Surface glyoxal concentrations are reported unless otherwise noted.

Name	Latitude	Longitude	Period	Hour of Day	Glyoxal (ppt)	Reference
Ocean						
Salt Point	39°N	123°W	Aug Sep 2005	11–14 Local time	20	Seaman et al. (2006)
Carribean Sea	15°N	66°W	Oct 1988	Daily mean	40	Zhou and Mopper (1990)
Sargasso Sea coast	15°N–27°N	94°W–66°W	Oct 1988 Mar 1989	Daily mean	80	Zhou and Mopper (1990)
Tropical Pacific NH	5°N–20°N	133°W–110°W	Jan Mar 2012	Daily mean	32	Coburn et al. (2014)
Tropical Pacific SH	5°S–10°S	110°W–93°W	Jan Mar 2012	Daily mean	43	Coburn et al. (2014)
TP NH aircraft RF12	8.5°N	101.5°W	Jan Feb 2012	Daily mean	25	Volkamer et al. (2015), 0–2 km mean
TP NH aircraft RF17	6°N–7°N	90°W–92°W	Jan Feb 2012	Daily mean	34	Volkamer et al. (2015), 0–2 km mean
Cape Grim	40°S–44°S	140°E–144°E	Aug Sep 2011	Daily mean	7	Lawson et al. (2015)
Chatham Rise	40°S–50°S	175°E–175°W	Feb Mar 2012	Daily mean	23	Lawson et al. (2015)
Tropical Eastern Pacific Ocean	15°S–5°N	85°W–95°W	Nov 2008 Jan 2009	Daily mean	67	Sinreich et al. (2010)
Cape Verde	17°N	25°W	Jun Sep 2014	Daily mean	5.6	Walker et al. (2022)
North Atlantic	40°N–70°N	10°W–10°E	Sep Oct 2017	Daily mean	19	Kluge et al. (2023), 0–2 km mean
Tropical Atlantic	6°S–35°N	40°W–3°E	Aug 2018	Daily mean	44	Kluge et al. (2023), 0–2 km mean
East China Sea	17°N–33°N	122°E–135°E	Mar 2018	Daily mean	75	Kluge et al. (2023), 0–2 km mean
Weddell Sea	43°S–60°S	34°W–75°W	Oct 2019	Daily mean	10	Kluge et al. (2023), 0–2 km mean
Land						
Amazon	12°S–2°N	51°W–68°W	Sep 2014	Daily mean	87	Kluge et al. (2020), 0–2 km mean
Hong Kong	22.217°N	114.25°E	Nov 2020 Feb 2021	10–15 Local time	45	Xu et al. (2023)
Xingtai	37.18°N	114.37°E	Aug 2021	6–18 LT	80	Wang et al. (2019)
Shenzhen	22.55°N	114.60°E	Sep Oct 2019	Daily mean	289	Zhu et al. (2021)
Guangzhou	23°N	113.2°E	Sep Nov 2018	Daily mean	1	Wu et al. (2020)
Hua Guo Shan	22.728°N	112.929°E	Jan 2017	Daily mean	100	Chang et al. (2019)
Mt. Hua	34.48°N	110.08°E	Aug 2020	Daily mean	330	Zhang et al. (2024)
Tazhong	38.97°N	83.66°E	May Jun 2018	Daily mean	210	Geng et al. (2022)
Mt. Hua	34.48°N	110.083°E	Aug 2020	Daily mean	260	Qi et al. (2023)
Shanghai	31.34°N	121.51°E	Jun Aug 2018	Daily mean	162	Guo et al. (2021)
Mt. Fuji-May	32.81°N	130.73°E	May 2016	Daily mean	30	Mitsuishi et al. (2018)
Mt. Fuji-Dec	32.81°N	130.73°E	Dec 2016	Daily mean	5	Mitsuishi et al. (2018)
Sierra Nevada Mountains	38.88°N	120.62°W	Jul 2009	Daily mean	33	DiGangi et al. (2012)
Mexico City	19.5°N	99°W	Apr 2003	Daily mean	270	Volkamer et al. (2007)

(Continued)

Table S1. Observed surface or boundary layer mean glyoxal concentration over land and ocean. (Continued)

Name	Latitude	Longitude	Period	Hour of Day	Glyoxal (ppt)	Reference
Shanghai	31.19°N	121.43°E	May Jun 2021	Daily mean	0.6	Chen et al. (2025), below detection limit
Hefei-MAM	31.78°N	117.2°E	Mar 2018 May 2018	8–17 Local time	230	Hong et al. (2022)
Hefei-JJA	31.78°N	117.2°E	Jun 2018 Aug 2018	8–17 Local time	220	Hong et al. (2022)
Hefei-SON	31.78°N	117.2°E	Sep 2018 Nov 2018	8–17 Local time	220	Hong et al. (2022)
Hefei-DJF	31.78°N	117.2°E	Dec 2018 Feb 2019	8–17 Local time	230	Hong et al. (2022)
Elizabeth-MAM	40.66°N	74.21°W	Mar May 2000 2001	Daily mean	718	Liu et al. (2006)
Elizabeth-JJA	40.66°N	74.21°W	Jun Aug 1999 2000	Daily mean	706	Liu et al. (2006)
Elizabeth-SON	40.66°N	74.21°W	Sep Nov 1999 2000	Daily mean	509	Liu et al. (2006)
Elizabeth-DJF	40.66°N	74.21°W	Dec Feb 1999 2001	Daily mean	448	Liu et al. (2006)
Lhasa	29.63°N	91.02°E	Aug 2000	Daily mean	400	Li et al. (2022)
Madrid-MAM	40.44°N	3.69°E	Mar 2016 May 2016	9 Local time	1410	Benavent et al. (2019)
Madrid-JJA	40.44°N	3.69°E	Jun 2016 Aug 2016	9 Local time	1040	Benavent et al. (2019)
Madrid-SON	40.44°N	3.69°E	Sep 2016 Nov 2016	9 Local time	980	Benavent et al. (2019)
Madrid-DJF	40.44°N	3.69°E	Dec 2016 Jan Feb 2016	9 Local time	1400	Benavent et al. (2019)
Chongqing	29.83°N	107.01°E	Dec 2018 Jan 2019	9–16 Local time	80	Xing et al. (2020)
Montelibretti	42.11°N	12.63°E	Jul Sep 2005	8–16 Local time	440	Possanzini et al. (2007)
Palaiseau-summer	48.71°N	2.21°E	Jul 2009	Daily mean	47	Ait-Helal et al. (2014)
Palaiseau-winter	48.71°N	2.21°E	Jan Feb 2010	Daily mean	158	Ait-Helal et al. (2014)
Rio de Janeiro-May	22.86°N	43.26°W	May 1999	Daytime	201	Grosjean et al. (2002)
Rio de Janeiro-JJA	22.86°N	43.26°W	Jul Aug 2000	Daytime	126	Grosjean et al. (2002)
Rio de Janeiro-SON	22.86°N	43.26°W	Sep Nov 2000	Daytime	99	Grosjean et al. (2002)
Blodgett Forest	38.9°N	120.63°W	Aug Sep 2000	8–21 Local time	27	Spaulding et al. (2003)
Bukit Atur	4.8°N	117.83°E	Apr Jul 2008	Daily mean	335	MacDonald et al. (2012)
Mt. Tai	36.25°N	117.1°E	Jun 2006	Daily mean	188	Kawamura et al. (2013)
Tomakomai Forest	42.73°N	141.52°E	Sep 2003	Daily mean	27	Ieda et al. (2006)
Melbourne-MAM	37.69°S	144.95°E	Mar May 2017 2019	6–17 Local time	164	Fayad et al. (2020)
Melbourne-JJA	37.69°S	144.95°E	Jun Aug 2017 2018	6–17 Local time	139	Fayad et al. (2020)
Melbourne-SON	37.69°S	144.95°E	Sep Nov 2017 2018	6–17 Local time	142	Fayad et al. (2020)
Melbourne-DJF	37.69°S	144.95°E	Dec Feb 2016 2019	6–17 Local time	134	Fayad et al. (2020)
Beijing	39.9°N	116.41°E	Jun 2017	Daily mean	116	Liang et al. (2013)
Los Angeles	34°N	118°W	Jun 2017	Daily mean	103	Washenfelder et al. (2011)
Manitou Forest	39°N	105°W	May Jun 2010	Daily mean	28	Wolfe et al. (2014)
Madison	43°N	89°W	Aug 2010	Daily mean	38	Henry et al. (2012)
Alabama	33°N	87°W	May 2011	Daily mean	29	Kaiser et al. (2016)
SOAS	33°N	87°W	Jun Jul 2013	Daily mean	33	Hettiyadura et al. (2017)
Northern Michigan	45.5°N	84.72°W	Jun Jul 2013	Daily mean	30	Johnson et al. (2008)
Simcoe	43°N	80°W	Jul 2008	Daily mean	500	Aiello et al. (2009)
Wuhan	31°N	114°E	Aug 2021	Daily mean	420	Huang et al. (2023)
Amazon-DJF	2.1°S	59°W	Dec 2019 Feb 2020	Daily mean	70	Donner et al. (2024)
Amazon-MAM	2.1°S	59°W	Mar May 2020	Daily mean	55	Donner et al. (2024)
Amazon-JJA	2.1°S	59°W	Jun Aug 2019	Daily mean	69	Donner et al. (2024)
Amazon-SON	2.1°S	59°W	Sep Nov 2019	Daily mean	80	Donner et al. (2024)

R1.15 Figure 2: Please add the respective references for the observations.

Thank you for the suggestion. We added Table S1 listing the details of all observations and added their respective references, as shown above.

R1.16 Line 202: This is not directly intuitive, considering that the model underestimates glyoxal in these bVOC source regions. How do you interpret an isoprene overestimation while at the same time glyoxal underestimation over regions clearly dominated by biogenic emissions? Is the model bias larger or smaller over bVOC source regions compared to other latitudes?

Thank you for this very important feedback. We added a new Figure S5 comparing the simulated surface isoprene concentrations in the standard and revised models to the observations in key biogenic regions. We found that, by applying the top-down constraints on regional isoprene emissions based on CrIS isoprene observations, the

simulated surface isoprene concentrations became closer to independent observations. This lent support for the regional scaling of isoprene emissions. However, the simulated regional glyoxal VCDs were impacted by both biogenic isoprene emissions and biomass burning emissions. Over South America, for example, our regional scaling reduced isoprene emissions, but simulated glyoxal VCDs increased as a result of increased biomass burning emissions.

[Main text, Section 6]: *Figure 2a compares simulated glyoxal concentrations against surface measurements over land. Excluding measurements from urban and biomass-burning sites, the GC-TM-EC simulation showed substantially better agreement with observations over land (NMB = –43%) than the GC-CTRL simulation (NMB = –77%). We found that this improvement over land arose not only from refined isoprene emissions and its glyoxal production, but also from a better quantification of glyoxal and its precursors from biomass burning. Figure 7 compares satellite-observed and simulated VCDs of glyoxal and isoprene, along with the observed and simulated glyoxal-isoprene ratios (R_{GI}) over four high-glyoxal regions. Figure S5 compares the simulated surface isoprene concentrations against measurements in key biogenic source regions. Over North America, the CrIS constraints on isoprene emissions corrected the low bias in GC-CTRL-simulated isoprene VCDs, improving the agreement with observed surface isoprene concentrations, while also improving the agreement between the simulated glyoxal VCDs and the TROPOMI observations. Updates in chemical mechanisms further improved the simulated glyoxal abundances and the R_{GI}, indicating a better representation of glyoxal production from isoprene. In contrast, over South America, Africa, and Southeast Asia, CrIS constraints either reduced or only slightly increased isoprene emissions, which brought the simulated surface isoprene concentrations to better agree with measurements (Figure S5). However, the enhanced biomass-burning emissions of glyoxal and its precursors substantially raised both the simulated glyoxal abundances and the simulated R_{GI} to become more consistent with observations. Chemical mechanism updates in GC-TM-EC only brought minor adjustments to simulated glyoxal abundance over these regions.*

These results underscore the large contribution of biomass burning emissions to atmospheric glyoxal, which must be better constrained to enable accurate NMVOC emission inversions using glyoxal VCDs.

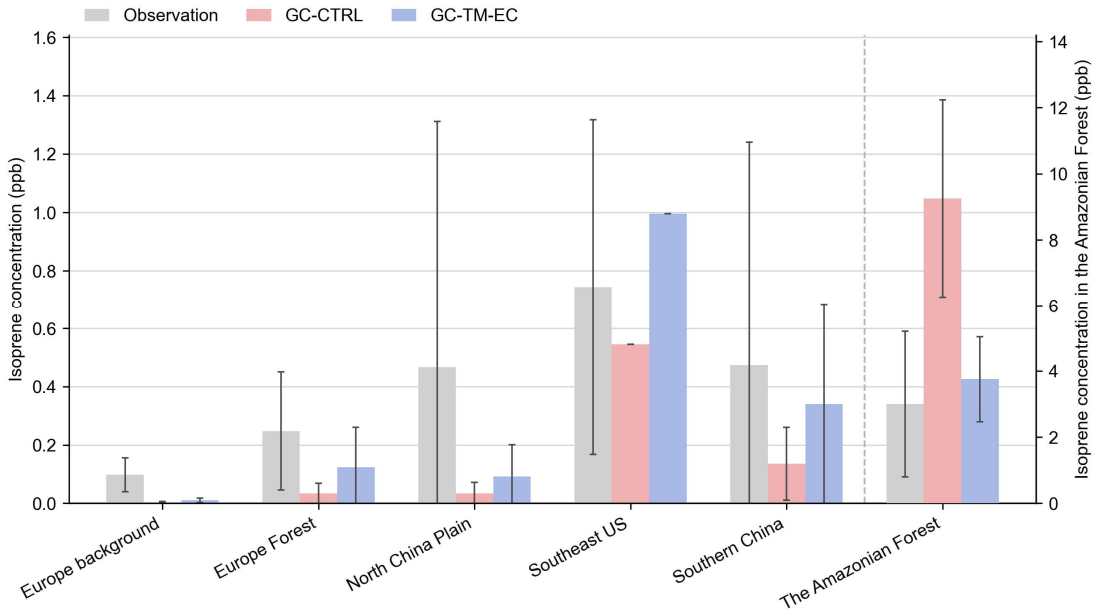

Figure S5. *Evaluations of GEOS-Chem simulated surface isoprene concentrations (unit: ppb) against measurements in major source areas of biogenic isoprene: Europe background (Garg et al., 2026), Europe forest (Seco et al., 2011), Amazonian forest (Sun et al., 2025), North China Plain (Zhang et al., 2020), South China (Zhang et al., 2020) and Southeast US forest (Link et al., 2015). The Amazonian forest site is plotted on a separate linear axis because of its much higher concentration range.*

R1.17 Line 227: I am aware that isoprene observations are globally sparse and not routinely available, but how does this scaling approach impact the comparison to independent isoprene measurements? How does it compare to results from TROPOMI-based isoprene inversion approaches?

Thank you for this very important feedback. We added a new Figure S5 comparing the simulated surface isoprene concentrations in the standard and revised models to the

observations in key biogenic regions. We found that, by applying the top-down constraints on regional isoprene emissions based on CrIS isoprene observations, the simulated surface isoprene concentrations became closer to independent observations. This lent support for the regional scaling of isoprene emissions. We also compared our scaled isoprene emission estimates to the most recent inverse estimate of isoprene emissions (Sfendla et al., 2026) using formaldehyde and glyoxal VCDs from TROPOMI.

[Main text, Section 4.1]: *The top-down constrained global isoprene emission was 438 Tg yr^{-1}, similar to the default 449 Tg yr^{-1} in GC-CTRL (Table 1). However, over the Northern mid-latitudes, the regional annual mean isoprene emissions were scaled by factors of 1.2 to 3.5, with maximum increases over the temperate ecosystems of Europe and Asia. Conversely, over the tropical ecosystems of the Amazon, Africa, and Northern Australia, our use of CrIS constraints decreased the regional isoprene emissions by 10% to 60%. These CrIS-based constraints on global isoprene emissions were still lower than the global isoprene emission estimates (490 to 514 Tg yr^{-1}) independently derived by* Sfendla et al., (2026) *using TROPOMI formaldehyde and glyoxal retrievals.*

[Main text, Section 6]: *Figure 2a compares simulated glyoxal concentrations against surface measurements over land. Excluding measurements from urban and biomass-burning sites, the GC-TM-EC simulation showed substantially better agreement with observations over land (NMB = –43%) than the GC-CTRL simulation (NMB = –77%). We found that this improvement over land arose not only from refined isoprene emissions and its glyoxal production, but also from a better quantification of glyoxal and its precursors from biomass burning. Figure 7 compares satellite-observed and simulated VCDs of glyoxal and isoprene, along with the observed and simulated glyoxal-isoprene ratios (R_{GI}) over four high-glyoxal regions. Figure S5 compares the simulated surface isoprene concentrations against measurements in key biogenic source regions. Over North America, the CrIS constraints on isoprene emissions*

corrected the low bias in GC-CTRL-simulated isoprene VCDs, improving the agreement with observed surface isoprene concentrations, while also improving the agreement between the simulated glyoxal VCDs and the TROPOMI observations. Updates in chemical mechanisms further improved the simulated glyoxal abundances and the R_{GI}, indicating a better representation of glyoxal production from isoprene. In contrast, over South America, Africa, and Southeast Asia, CrIS constraints either reduced or only slightly increased isoprene emissions, which brought the simulated surface isoprene concentrations to better agree with measurements (Figure S5). However, the enhanced biomass-burning emissions of glyoxal and its precursors substantially raised both the simulated glyoxal abundances and the simulated R_{GI} to become more consistent with observations. Chemical mechanism updates in GC-TM-EC only brought minor adjustments to simulated glyoxal abundance over these regions. These results underscore the large contribution of biomass burning emissions to atmospheric glyoxal, which must be better constrained to enable accurate NMVOC emission inversions using glyoxal VCDs.

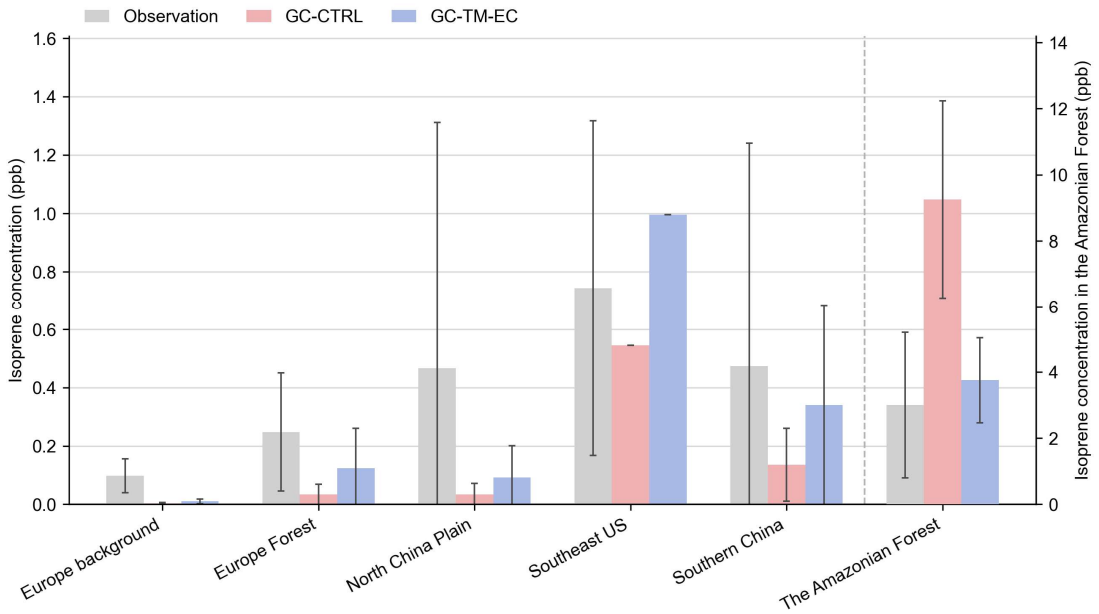

Figure S5. *Evaluations of GEOS-Chem simulated surface isoprene concentrations*

(unit: ppb) against measurements in major source areas of biogenic isoprene: Europe background (Garg et al., 2026), Europe forest (Seco et al., 2011), Amazonian forest (Sun et al., 2025), North China Plain (Zhang et al., 2020), South China (Zhang et al., 2020) and Southeast US forest (Link et al., 2015). The Amazonian forest site is plotted on a separate linear axis because of its much higher concentration range.

R1.18 Line 276: two-stages -> two stages

Corrected. Thank you.

R1.19 Line 280: ... and undergo rapid... ?

Thank you for pointing out this lack of clarity. We corrected the sentence:

[Main text lines 319-320]: *The first-generation production aligned with the theoretical pathways proposed by Dibble (2004a, b), wherein specific Z-δ-hydroxy-peroxy isoprene radicals (ISOPOO) first react with NO, then rapidly undergo 1,5 H-shifts and O_2-additions to yield dihydroxy peroxy radicals.*

R1.20 Line 281: fragments

Corrected. Thank you.

R1.21 Line 380: As above, considering this elevated isoprene-glyoxal yield in low NOx/high HOx environments, how do you interpret the model overestimation of isoprene coinciding with an underestimation of glyoxal in these regions?

Thank you for this very important feedback. The yield of glyoxal from isoprene in low-NO_x environments is still highly uncertain, and we revised the main text to emphasize this uncertainty. However, these low-NO_x regions often coincide with major forests, which are also susceptible to biomass burning. We found that the simulated regional glyoxal VCDs were impacted by both biogenic isoprene emissions and biomass burning

emissions. Over South America, for example, our regional scaling reduced isoprene emissions, but simulated glyoxal VCDs increased as a result of increased biomass burning emissions. We revised the text to more thoroughly discuss the impacts of biomass burning on several regions of underestimated glyoxal abundance.

[Main text, Section 5.1.3]: *Field observations in low-NO_x, isoprene-dominated environments indicated that glyoxal production from isoprene is likely substantial. Li et al. (2016) and Chan Miller et al. (2017) analyzed the Southeast Nexus (SENEX) aircraft campaign data over Southeast U.S. during summer 2013. Both studies demonstrated that the observed glyoxal levels and R_{GF} values in this lower-NO_x (0.05 to 0.1 ppb between 0 to 5 km altitude) environment could be well simulated using mechanisms where glyoxal yields at low NO_x were comparable or even exceeded those at high NO_x. Although the two studies proposed different chemical pathways to explain this phenomenon, their results consistently supported a sustained or potentially enhanced glyoxal yield under low-NO_x conditions, such as that in our revised mechanism and in the RCIM. However, a recent direct measurement reported a glyoxal yield of 0.52 ± 0.06% from OH-initiated isoprene oxidation under extremely low NO_x (<70 ppt) (Warman, 2024), contradicting the inference from field observations and underscoring significant uncertainties in quantifying low-NO_x glyoxal yields from isoprene.*

[Main text, Section 6]: *Figure 2a compares simulated glyoxal concentrations against surface measurements over land. Excluding measurements from urban and biomass-burning sites, the GC-TM-EC simulation showed substantially better agreement with observations over land (NMB = –43%) than the GC-CTRL simulation (NMB = –77%). We found that this improvement over land arose not only from refined isoprene emissions and its glyoxal production, but also from a better quantification of glyoxal and its precursors from biomass burning. Figure 7 compares satellite-observed and simulated VCDs of glyoxal and isoprene, along with the observed and simulated*

glyoxal-isoprene ratios (R_{GI}) over four high-glyoxal regions. Figure S5 compares the simulated surface isoprene concentrations against measurements in key biogenic source regions. Over North America, the CrIS constraints on isoprene emissions corrected the low bias in GC-CTRL-simulated isoprene VCDs, improving the agreement with observed surface isoprene concentrations, while also improving the agreement between the simulated glyoxal VCDs and the TROPOMI observations. Updates in chemical mechanisms further improved the simulated glyoxal abundances and the R_{GI}, indicating a better representation of glyoxal production from isoprene. In contrast, over South America, Africa, and Southeast Asia, CrIS constraints either reduced or only slightly increased isoprene emissions, which brought the simulated surface isoprene concentrations to better agree with measurements (Figure S5). However, the enhanced biomass-burning emissions of glyoxal and its precursors substantially raised both the simulated glyoxal abundances and the simulated R_{GI} to become more consistent with observations. Chemical mechanism updates in GC-TM-EC only brought minor adjustments to simulated glyoxal abundance over these regions. These results underscore the large contribution of biomass burning emissions to atmospheric glyoxal, which must be better constrained to enable accurate NMVOC emission inversions using glyoxal VCDs.

R1.22 Line 475: though a global bias

Corrected. Thank you.

R1.23 Line 526: were -> was

Corrected. Thank you.

R1.24 Line 591: the Amazonian rainforest

Corrected. Thank you.

Response to Anonymous Referee #2,

R2.1 Zhang et al present work investigating the atmospheric glyoxal budget using a combination of satellite data and GEOS-Chem modeling. This topic is important and addressing issues with modern understanding in this domain is a worthwhile effort. While the authors present a thorough analysis, I believe there are several key pitfalls in this work that warrant further attention before this manuscript should be accepted for publication. They are highlighted below.

We thank the reviewer for the thoughtful and rigorous comments on our manuscript. We address these comments point-by-point below. In particular, we have re-run all global GEOS-Chem simulations at 2.5° × 2° resolution and revised all diagnostics accordingly.

R2.2 Model resolution: 4˚x5˚ is very coarse spatial resolution and not at all state of the art. Existing work in GEOS-Chem routinely uses 2˚x2.5˚ or higher and has for the past several decades. Given that many of the spatial gradients in glyoxal concentrations are on the order of 10s of km or smaller, the authors need to justify why this resolution was chosen. The authors should explicitly discuss how and where a 4x5 degree simulation would be useful to modern atmospheric chemistry understanding, and consider of completing new simulations at 2˚x2.5˚.

Thank you for the suggestion. We have re-run all global GEOS-Chem simulations at 2.5° × 2° resolution and revised all diagnostics, Tables, and Figures accordingly. The change of model resolution affected the simulated

glyoxal budget by less than 5%. The main findings of the study were unchanged.

R2.3 Data-model agreement: GEOS-Chem and the satellite retrieval disagree by quite a lot in this work. The authors do highlight this. However given the enormous uncertainties in both the simulation and the satellite data, it is difficult to know what to take away from this work as a reader. Can you tell if the model right? Are the satellite data to be trusted? Is an NMB of 60% even high at all given the coarse resolution and huge observational uncertainty?

More detailed statistical treatment of the role of uncertainty in the satellite retrievals would strengthen this work substantially.

Thank you for this important comment. Our goal in this study is to combine current-best knowledge to improve the model representation of the emissions and chemistry of glyoxal and its precursors, such that assessments of their atmospheric impacts and more detailed inverse modeling may be realistically conducted. We acknowledge that much uncertainty remain in the sources and sinks of atmospheric glyoxal and its precursors, from both terrestrial and marine sources. We rewrote the conclusion section to highlight these uncertainties.

We also added model-observations comparisons of surface CO, ozone, isoprene, and SOA concentrations, as well as model-observations of vertical profiles of glyoxal and HO_2 concentrations over the remote oceans. **Please kindly refer to our responses to R1.4 and R1.5 above.** Together, the apparent improvements in simulated CO, ozone, and SOA should therefore be interpreted as supporting the chemical plausibility of the revised glyoxal budget and underscoring glyoxal's role as a proxy for atmospheric NMVOC emissions.

[Main text, Conclusion]: *Even with our improved precursor emission estimates and chemical representation, our simulated glyoxal remained approximately 40% lower than satellite glyoxal retrievals and surface observations over land. This discrepancy likely stems from both satellite retrieval uncertainties and persistent uncertainties in*

emissions and chemistry. Anthropogenic emissions of glyoxal precursors, particularly aromatic compounds, are variable and uncertain among different emission inventories and demonstrated a consistent low-bias compared to observations (Yan et al., 2019). In addition, while we scaled isoprene and biomass burning emissions by region on an annual basis, this approach may introduce biases across different land cover types and seasons (Silva et al., 2018; Wang et al., 2024; DiMaria et al., 2025). Uncertainties in simulated OH and NO_x concentrations may moderately affect glyoxal production, but they have a potentially large impact on top-down isoprene estimates, particularly over the Amazonian rainforest, where underestimated OH and NO_x lead to isoprene overestimation for a given emission rate (Wells, et al., 2020). Further uncertainties arise from incomplete representation of key chemical pathways, including glyoxal production from isoprene under low-NO_x conditions (Warman, 2024), ozonolysis via Criegee intermediates (Vansco et al., 2020), detailed isoprene nitrate chemistry (Schwantes et al., 2015), and heterogeneous uptake processes of glyoxal (Li et al., 2016; Kim et al., 2022).

Our study highlights the need for improved measurement of VOCs in the MBL and for a deeper exploration of their photochemical transformations. Our exploratory addition of a hypothetical secondary glyoxal source (66 Tg yr^{-1}) raised the global atmospheric glyoxal source to 106 Tg yr^{-1} and its burden to 39 Gg. While this addition shows tentative consistency with in situ MBL observations, this hypothetical glyoxal source cannot be explained by known marine precursor emissions. Recent work suggests marine biogenic emissions of precursors, such as isoprene, may be larger than previous estimates (Zhang et al., 2022). However, our evaluation of model results against limited aircraft measurements points to the possible influence of a more long-live precursor, the nature and impacts of which remain highly uncertain. Resolving this gap in marine photochemistry is essential for quantifying the roles of glyoxal and its precursors in marine and global atmospheric chemistry.

R2.4 Hypothetical Ocean Source: The GC-TM-EC simulation and related discussion

is missing a very important caveat. Namely that according to equation 3, the authors specifically scaled an ocean emissions term such that the model and satellite data agreed. Once this was done, the paper discusses how well the concentrations agree in Section 6. This is a circular argument.

Further, glyoxal retrievals over oceans often have quite large per-retrieval errors, the statistical implications of which are not discussed in nearly enough detail in this manuscript. There is deep literature discussing robust emissions estimation from uncertain satellite observations. Incorporation of that kind of work would strengthen this paper.

There may well be missing emissions of glyoxal from oceans in current models. This work does not provide particularly strong evidence in that direction. Instead, this work demonstrates that adding a hypothetical source of glyoxal over oceans based on extremely noisy satellite data does improve agreement with observations. A variety of prior papers have suggested as much. While that may be true, there are many other potential issues with the simulation of photooxidants that could lead to similar changes in concentrations.

Thank you for your detailed review and valuable comments. Here, our goal is to estimate how large that hypothetical glyoxal source might be given satellite constraints, and whether that estimated source is consistent with independent measurements. The marine glyoxal source introduced in our study is hypothetical but is tentatively supported by *in situ* and ground-based remote sensing measurements. We revised the main text to make the hypothetical nature more evident to readers. We also added discussion to elucidate the observational support for this hypothesis and explore its uncertainties.

[Main text, Section 4.3]:

TROPOMI and other in situ and remote sensing measurements tentatively implied a secondary source of glyoxal over the tropical MBL associated with unknown, potentially biogenic, marine precursors. In this work, we used TROPOMI observations

to estimate how large that hypothetical secondary glyoxal source might be, and we evaluated whether the inclusion of that hypothetical glyoxal source is consistent with independent in situ and remote sensing measurements in the global MBL. Previous studies have tentatively linked the glyoxal in the MBL to biologically active waters or to photochemical production from the dissolved organic matter (DOM) content in sea water. However, currently reported concentrations or fluxes of precursors (e.g., isoprene, ethylene, and propene) appear insufficient to explain the magnitude of glyoxal inferred from satellite observations (Broadgate et al., 2004; Zhang et al., 2025; Pound, 2021). In addition, measurements of NMVOCs in the MBL remain too sparse to provide a quantitative global constraint. We therefore interpret the inferred marine glyoxal source as a diagnostic term representing the glyoxal production from potentially missing marine NMVOCs.

[Main text, Section 6]: *Figure S4 further compares the simulated glyoxal over the remote ocean with the aircraft observations from Volkamer et al. (2015) and Kluge et al. (2023). With the added marine glyoxal source, GC-TM-EC-simulated glyoxal concentrations aligned better with the limited aircraft data. However, the model overestimated glyoxal in surface air over the Northeast Pacific but underestimated it over the Atlantic. Additionally, the aircraft profiles suggested a more gradual decline in glyoxal concentration with altitude than simulated, which may indicate a longer-lived marine-derived precursor. This inference is inconsistent with the current understanding that marine-emitted VOCs are predominantly short-lived alkenes (e.g., ethylene and propene) and isoprene (Broadgate et al., 2004; Zhang et al., 2025; Pound, 2021).*

[Main text, Conclusion]:

Our study highlights the need for improved measurement of VOCs in the MBL and for a deeper exploration of their photochemical transformations. Our exploratory addition

of a hypothetical secondary glyoxal source (66 Tg yr^{-1}) raised the global atmospheric glyoxal source to 106 Tg yr^{-1} and its burden to 39 Gg. While this addition shows tentative consistency with in situ MBL observations, this hypothetical glyoxal source cannot be explained by known marine precursor emissions. Recent work suggests marine biogenic emissions of precursors, such as isoprene, may be larger than previous estimates (Zhang et al., 2022). However, our evaluation of model results against limited aircraft measurements points to the possible influence of a more long-live precursor, the nature and impacts of which remain highly uncertain. Resolving this gap in marine photochemistry is essential for quantifying the roles of glyoxal and its precursors in marine and global atmospheric chemistry.

References

Broadgate, W. J., Malin, G., Küpper, F. C., Thompson, A., & Liss, P. S. (2004). Isoprene and other non-methane hydrocarbons from seaweeds: A source of reactive hydrocarbons to the atmosphere. *Marine Chemistry*, *88*(1), 61–73. (132). https://doi.org/10.1016/j.marchem.2004.03.002

Chen, X., Wang, N., Wang, G., Wang, Z., Chen, H., Cheng, C., Li, M., Zheng, L., Wu, L., Zhang, Q., Tang, M., Huang, B., Wang, X., & Zhou, Z. (2022). The Influence of Synoptic Weather Patterns on Spatiotemporal Characteristics of Ozone Pollution Across Pearl River Delta of Southern China. *Journal of Geophysical Research: Atmospheres*, *127*(21), e2022JD037121. https://doi.org/10.1029/2022JD037121

Ferracci, V., Weber, J., Bolas, C. G., Robinson, A. D., Tummon, F., Rodríguez-Ros, P., Cortés-Greus, P., Baccarini, A., Jones, R. L., Galí, M., Simó, R., Schmale, J., & Harris, Neil. R. P. (2024). Atmospheric isoprene measurements reveal larger-than-expected Southern Ocean emissions. *Nature Communications*, *15*(1), 2571. (6). https://doi.org/10.1038/s41467-024-46744-4

Kelly, J. M., Doherty, R. M., O'Connor, F. M., & Mann, G. W. (2018). The impact of

biogenic, anthropogenic, and biomass burning volatile organic compound emissions on regional and seasonal variations in secondary organic aerosol. *Atmospheric Chemistry and Physics*, *18*(10), 7393–7422. https://doi.org/10.5194/acp-18-7393-2018

Li, J.-L., Zhai, X., Wu, Y.-C., Wang, J., Zhang, H.-H., & Yang, G.-P. (2021). Emissions and potential controls of light alkenes from the marginal seas of China. *Science of The Total Environment*, *758*, 143655. (13). https://doi.org/10.1016/j.scitotenv.2020.143655

Müller, J.-F., Stavrakou, T., & Peeters, J. (2019). Chemistry and deposition in the Model of Atmospheric composition at Global and Regional scales using Inversion Techniques for Trace gas Emissions (MAGRITTE v1.1) – Part 1: Chemical mechanism. *Geoscientific Model Development*, *12*(6), 2307–2356. (46). https://doi.org/10.5194/gmd-12-2307-2019

Pound, R. J. (2021). *Quantifying the importance of ocean-atmosphere exchange for atmospheric chemistry* [Phd, University of York]. https://etheses.whiterose.ac.uk/id/eprint/29608/

Sfendla, Y., Stavrakou, T., Müller, J.-F., Oomen, G.-M., Opacka, B., Danckaert, T., De Smedt, I., & Lerot, C. (2026). Global VOC emissions quantified from inversion of TROPOMI spaceborne formaldehyde and glyoxal data. *Atmospheric Chemistry and Physics*, *26*(1), 733–767. https://doi.org/10.5194/acp-26-733-2026

Song, S., Ma, T., Zhang, Y., Shen, L., Liu, P., Li, K., Zhai, S., Zheng, H., Gao, M., Moch, J. M., Duan, F., He, K., & McElroy, M. B. (2021). Global modeling of heterogeneous hydroxymethanesulfonate chemistry. *Atmospheric Chemistry and Physics*, *21*(1), 457–481. (28). https://doi.org/10.5194/acp-21-457-2021

Spracklen, D. V., Jimenez, J. L., Carslaw, K. S., Worsnop, D. R., Evans, M. J., Mann, G. W., Zhang, Q., Canagaratna, M. R., Allan, J., Coe, H., McFiggans, G., Rap, A., & Forster, P. (2011). Aerosol mass spectrometer constraint on the global

secondary organic aerosol budget. *Atmospheric Chemistry and Physics*, *11*(23), 12109–12136. https://doi.org/10.5194/acp-11-12109-2011

Tripathi, N., Sahu, L. K., Singh, A., Yadav, R., Patel, A., Patel, K., & Meenu, P. (2020). Elevated Levels of Biogenic Nonmethane Hydrocarbons in the Marine Boundary Layer of the Arabian Sea During the Intermonsoon. *Journal of Geophysical Research: Atmospheres*, *125*(22), e2020JD032869. (21). https://doi.org/10.1029/2020JD032869

Volkamer, R., Baidar, S., Campos, T. L., Coburn, S., DiGangi, J. P., Dix, B., Eloranta, E. W., Koenig, T. K., Morley, B., Ortega, I., Pierce, B. R., Reeves, M., Sinreich, R., Wang, S., Zondlo, M. A., & Romashkin, P. A. (2015). Aircraft measurements of BrO, IO, glyoxal, NO_2, H_2O, O_2–O_2 and aerosol extinction profiles in the tropics: Comparison with aircraft-/ship-based in situ and lidar measurements. *Atmospheric Measurement Techniques*, *8*(5), 2121–2148. https://doi.org/10.5194/amt-8-2121-2015

Wang, R., Shen, H., Zeng, C., Chen, J., Wang, Y., & Li, Y. (2025). A global land daily 10-km-resolution surface ozone dataset from 2013–2022. *Scientific Data*, *12*(1), 1710. (1). https://doi.org/10.1038/s41597-025-05990-x

Waxman, E. M., Elm, J., Kurtén, T., Mikkelsen, K. V., Ziemann, P. J., & Volkamer, R. (2015). Glyoxal and Methylglyoxal Setschenow Salting Constants in Sulfate, Nitrate, and Chloride Solutions: Measurements and Gibbs Energies. *Environmental Science & Technology*, *49*(19), 11500–11508. (67). https://doi.org/10.1021/acs.est.5b02782

Wells, K. C., Millet, D. B., Payne, V. H., Deventer, M. J., Bates, K. H., de Gouw, J. A., Graus, M., Warneke, C., Wisthaler, A., & Fuentes, J. D. (2020). Satellite isoprene retrievals constrain emissions and atmospheric oxidation. *Nature*, *585*(7824), 225–233. (75). https://doi.org/10.1038/s41586-020-2664-3

Wu, Y.-C., Li, J.-L., Wang, J., Zhuang, G.-C., Liu, X.-T., Zhang, H.-H., & Yang, G.-P.

(2021). Occurance, emission and environmental effects of non-methane hydrocarbons in the Yellow Sea and the East China Sea. *Environmental Pollution*, *270*, 116305. (17). https://doi.org/10.1016/j.envpol.2020.116305

Xie, X., Zhang, Y., Liang, R., & Wang, X. (2025). Global modeling of brown carbon: Impact of temperature- and humidity-dependent bleaching. *Atmospheric Chemistry and Physics*, *25*(20), 13547–13561. https://doi.org/10.5194/acp-25-13547-2025

Zhang, W., & Gu, D. (2022). Geostationary satellite reveals increasing marine isoprene emissions in the center of the equatorial Pacific Ocean. *Npj Climate and Atmospheric Science*, *5*(1), 83. https://doi.org/10.1038/s41612-022-00311-0

Zhang, W., Weber, J., Archibald, A. T., Abraham, N. L., Booge, D., Yang, M., & Gu, D. (2025). Global Atmospheric Composition Effects from Marine Isoprene Emissions. *Environmental Science & Technology*, *59*(5), 2554–2564. (1). https://doi.org/10.1021/acs.est.4c10657